Investigation of Microbial Electrochemical Cell (MEC) as a Sustainable Alternative for Synthesizing Hydrogen Peroxide (H_2O_2)

by

Junyoung Justin Sim

A thesis

presented to the University of Waterloo

in fulfillment of the

thesis requirement for the degree of

Master of Applied Science

in

Civil Engineering

Waterloo, Ontario, Canada, 2014

AUTHOR'S DECLARATION

I hereby declare that I am the sole author of this thesis. This is a true copy of the thesis, including any required final revisions, as accepted by my examiners.

I understand that my thesis may be made electronically available to the public.

Junyoung Justin Sim

ABSTRACT

Hydrogen peroxide (H_2O_2) is an environmentally-safe strong oxidant that has many practical applications. While H_2O_2 is capable of oxidizing a variety of contaminants, its end products are only H_2O and O_2. As a result, the world-wide demand for H_2O_2 is growing significantly. To meet the high demand, H_2O_2 is exclusively manufactured through the *anthraquinone oxidation* (AO) process due to its ability to produce highly concentrated H_2O_2. However, the AO process requires high energy consumption and additional costs (transportation, storage, and handling), and the search for a more sustainable H_2O_2 production method is on-going. Microbial electrochemical cell (MEC) has shown its potential as an alternative sustainable method for H_2O_2 production. MEC is an emerging biotechnology that can produce H_2O_2 from wastewater by marrying microbial metabolism with oxygen reduction reaction (ORR) in electrochemical cells. Although a few past studies demonstrated H_2O_2 production in lab-scale MECs, they only presented a proof-of-concept. Therefore, this study was carried out to assess the feasibility of the MECs for H_2O_2 production with the objectives to (1) establish the optimal operation conditions for H_2O_2 production, (2) to evaluate H_2O_2 production and wastewater treatment in a lab-scale MEC under different operating conditions (feed and hydraulic residence time), and (3) to investigate the feasibility of H_2O_2 production in a pilot-scale MEC.

Preliminary experiments were conducted to establish the optimal operating conditions for the cathode of MECs. In the experiments, H_2O_2 production was compared for cathode materials (the graphite cathode vs the carbon gas diffusion cathode) and aeration methods (active aeration vs passive aeration) within a range of the $E_{cathode}$. In the experiment, the carbon gas diffusion cathode resulted in higher H_2O_2 production than the graphite cathode when the active aeration was implemented for the cathode, although O_2 reduction to H_2O was dominant over O_2 reduction to

H_2O_2 at all $E_{cathode}$. However, O_2 reduction to H_2O_2 improved significantly at all $E_{cathode}$ when passive air diffusion was employed for the carbon gas diffusion cathode. Therefore, it was determined that H_2O_2-producing MEC should be equipped with the carbon gas diffusion cathode and the passive aeration for the cathode for the optimal H_2O_2 production.

In the following experiments, a lab-scale MEC was operated on two feeds (acetate-fed MEC vs wastewater-fed MEC) under various hydraulic residence times (HRTs). Both acetate-MEC and wastewater-MEC showed efficient degradation of organics in each feed; the acetate-fed MEC achieved the COD removal efficiency of 45 ± 2 to 94 ± 2 % for a range of HRTs from 2 to 24 hrs when the wastewater-fed MEC achieved the COD removal efficiency of 39 ± 7 to 64 ± 5 % for a range of HRT from 2 to 10 hrs. However, a significant amount of the COD removed in the acetate-fed MEC was converted to current while most of the organics in the wastewater-fed MEC was converted to electron sinks, such as methane. As a result, higher current density and H_2O_2 production was observed in the acetate-MEC. The highest current density of 8 ± 0.56 A/m^2 and the highest cumulative H_2O_2 concentration of 843.50 ± 17.30 mg/L at 6 hr of cathode operation were achieved in the acetate-fed MEC. However, the highest current density of 0.56 ± 0.05 A/m^2 was observed in the wastewater-fed MEC, resulting in a cumulative H_2O_2 concentration of 147.73 ± 1.98 mg/L at 24 hr of cathode operation.

Finally, a pilot-scale MEC was operated on acetate synthetic wastewater with a different ion exchange membrane (AEM-MEC vs CEM-MEC). The current density in the pilot-scale MEC was 0.94 A/m^2 in the AEM-MEC and 0.96 A/m^2 in the CEM-MEC. As a result of low current densities in the pilot-scale MEC, low H_2O_2 production was observed; a cumulative H_2O_2 concentration was 9.0 ± 0.38 mg/L in the 20-day operation of the AEM-MEC and 98.48 ± 1.6 mg/L in the 16-day

operation of the CEM-MEC. Also, low H_2O_2 conversion efficiency of 0.35 ± 0.05 and 7.2 ± 0.09 % in the AEM-MEC and CEM-MEC, respectively was observed due to high pH in the cathode and low H_2O_2 production rate. In addition, technical and design challenges were identified in the pilot-scale MEC: membrane expansion, CO_2 trapping due to the absence of an outlet, and positioning of carbon gas diffusion cathode. These challenged had an adverse effect on the performance of the pilot system. These results highlight that the future research is required to improve current generation and H_2O_2 production in large-scale MECs while coping with the identified challenges.

ACKNOWLEDGEMENTS

I would like to express my gratitude to my supervisor Dr. Hyung-Sool Lee for his help and guidance over the entire course of my study. He enlightened me with his knowledge and expertise in the field of wastewater treatment engineering, and helped me to complete my research with his patient guidance and support. I am very privileged to have spent two years learning about the technology that holds a promising potential in the future. I also would like to gratefully acknowledge the useful advice and guidance of Dr. Jun-yeong An and Dr. Elsayed Elbeshbishy. You really helped me get through the challenge and hardship that I encountered on a daily-basis throughout the course of the graduate program. Furthermore, I would like to show my appreciation towards Dr. Monica B. Emelko and Dr. Hassan Baaj for taking their time to review my thesis.

My special gratitude goes to Mark Sobon and Mark Merlau of Civil and Environmental Engineering department for their technical supports on a number of occasions. I am also very grateful for the financial support provided by the University of Waterloo and the Natural Sciences and Engineering Research Council of Canada (NSERC).

I would like to thank all the colleagues in Waterloo Environmental Biotechnology Laboratory (WEBL) for their supports and friendship. It was my pleasure to work with you in the lab.

Lastly, I would like to thank all my family and friends in Korea and Canada. You guys helped me stay motivated and focused along this journey.

TABLE OF CONTENTS

AUTHOR'S DECLARATION ii

ABSTRACT iii

ACKNOWLEDGEMENTS vi

LIST OF FIGURES x

LIST OF TABLES xii

LIST OF ABBREVIATIONS AND NOMENCLATURE xiii

1. Introduction 1

1.1 Background 1

1.2 Microbial Electrochemical Cell (MEC) 2

1.2.1 Fundamental Electrochemistry in MECs 3

1.2.2 H_2O_2-producing MEC 6

1.3 Research Objectives 7

1.4 Research Map 7

1.5 Thesis Organization 8

2. Investigating the effect of cathodic parameters on the electrochemical generation of H_2O_2: cathode potential, cathode material, and aeration method 9

2.1 Introduction 10

2.2 Materials & Methods 13

2.2.1 Reactor Configuration 13

2.2.2 Operating Conditions 14

2.2.3 Analytical methods and Computation 15

2.3 Results & Discussion 16

2.3.1 Graphite Cathode vs Carbon Gas Diffusion Cathode under Active Aeration 16

2.3.2 Carbon Gas Diffusion Cathode under Passive Air Diffusion 18

2.4 Conclusions 21
3. H_2O_2 Production in a Laboratory-scale Microbial Electrochemical Cell 23
3.1 Introduction 25
3.2 Material & Method 27
3.2.1 Reactor Configuration 27
3.2.2 Inoculation and Start-up 29
3.2.3 Operation 30
3.2.4 Analytical method and Computation 31
3.3 Results & Discussion 32
3.3.1 Lab-scale MEC fed with Acetate Synthetic Wastewater 32
3.3.1.1 Current Generation & COD Removal 32
3.3.1.2 H_2O_2 Concentration & H_2O_2 Conversion Efficiency 34
3.3.2 Lab-scale MEC fed with Domestic Wastewater 38
3.3.2.1 Current generation & COD removal 38
3.3.2.2 H_2O_2 Concentration & H_2O_2 Conversion Efficiency 39
3.4 Conclusions 41
4. H_2O_2 production in a pilot-scale Microbial Electrochemical Cell 43
4.1 Introduction 44
4.1 Material & Method 45
4.1.1 Reactor Configuration 45
4.1.2 Operation 48
4.1.3 Analytical method and Computation 49
4.2 Results & Discussion 50
4.2.1 Cell Voltage, Anode & Cathode Potential, and Current Density 50
4.2.2 COD Removal Efficiency 54

4.2.3 pH & Conductivity 56
4.3 Conclusions 62
5 Conclusions 64
6 Recommendations 67
References 68
Appendix A: H_2O_2 Evolution in the laboratory-scale MEC fed with acetate 75

LIST OF FIGURES

Figure 1.1: A typical configuration of a dual-chamber Microbial Electrochemical Cell. 3
Figure 2.1: An electrochemical cell built for the preliminary experiments. 13
Figure 2.2: Average current density (left) and cell voltage (right) for both cathodes in phase I.. 16
Figure 2.3: Cumulative H_2O_2 concentration in 180-min operation in phase I for GC (left) and CGC (right). 17
Figure 2.4: H_2O_2 conversion efficiency over 180-min operation for GC (left) and CGC (right) in phase I. 18
Figure 2.5: Average current density (left) and the cell voltage (right) in phase II. 19
Figure 2.6: Cumulative H_2O_2 concentration in 180-min operation in phase II. 20
Figure 2.7: H_2O_2 conversion efficiency evolution in 180-min in phase II. 21
Figure 3.1: Picture (left) and the schematic diagram (right) of the lab-scale MEC..... 27
Figure 3.2: An anode module incorporated into the lab-scale MEC 28
Figure 3.3: Cell voltage (left) and the cathode potential (right) against current density in the acetate-fed MEC at different HRTs. 33
Figure 3.4: Cumulative H_2O_2 concentration and H_2O_2 conversion efficiency at 6 hr of the cathode operation in the acetate-fed MEC at different HRTs. 35
Figure 3.5: Cumulative H_2O_2 concentration and H_2O_2 conversion efficiency after 24 hrs of cathode operation in the acetate-fed MEC at different HRTs. 36
Figure 3.6: Cell voltage (left) and cathode potential (right) against current density in the wastewater-MEC at a different HRT. 38
Figure 3.7: Cumulative H_2O_2 concentration and H_2O_2 conversion efficiency at 6 hr and 24 hr of the cathode operation for the wastewater-MEC at different HRTs. 40
Figure 4.1: Schematic diagram (left) and the picture (right) of the pilot-scale MEC..... 45
Figure 4.2: Membrane expansion in the pilot-scale MEC (left) and proposed membrane supports (right). 46
Figure 4.3: Schematic diagram of the anode chamber (left) and the picture of the anode panel (right). 47
Figure 4.4: Cell voltage and electrode potential in the AEM-MEC. 50
Figure 4.5: Cell voltage and electrode potential in the CEM-MEC. 50

Figure 4.6: Water evaporation over time in the cathode compartment51
Figure 4.7: Current density in the 20-day operation of AEM-MEC..... 52
Figure 4.8: Current density in the 16-day operation of the CEM-MEC 53
Figure 4.9: Influent and effluent COD concentration in the AEM-MEC. 55
Figure 4.10: Influent and effluent COD concentration in the CEM-MEC. 55
Figure 4.11: Anolyte and catholyte pH in the AEM-MEC. 56
Figure 4.12: Anolyte and catholyte pH in the CEM-MEC. 56
Figure 4.13: CO_2 released to the air in the lab-scale MEC and CO_2 trapped in the pilot-scale MEC 58
Figure 4.14: Anolyte and catholyte conductivity in the AEM-MEC. 59
Figure 4.15: Anolyte and catholyte conductivity in the CEM-MEC. 59
Figure 4.16: H_2O_2 concentration and H_2O_2 conversion efficiency in the AEM-MEC. 60
Figure 4.17: H_2O_2 concentration and H_2O_2 conversion efficiency in the CEM-MEC. 61
Figure A.0.1: H_2O_2 concentration and conversion efficiency evolution in the laboratory-scale MEC fed with acetate at different HRTs. 76

LIST OF TABLES

Table 3.1: COD concentration in the influent and the effluent, COD removal efficiency (R_t) and coulombic efficiency at different HRTs. 34
Table 3.2: Change in the catholyte pH over 24 hr-operation of the acetate-fed MEC at different HRTs. 37
Table 3.3: COD concentration in the influent and the effluent, COD removal efficiency and coulombic efficiency in the wastewater-MEC at different HRTs 39
Table 3.4: Change in the catholyte pH over 24 hr of operation of the wastewater-fed MEC at different HRTs. 41

LIST OF ABBREVIATIONS AND NOMENCLATURE

AEM: Anion Exchange Membrane

AO: Anthraquinone Oxidation

ARB: Anode-Respiring Bacteria

CEM: Cation Exchange Membrane

CGC: Carbon Gas diffusion Cathode

COD: Chemical Oxygen Demand

E_{anode}: Anode potential

$E_{cathode}$: Cathode potential

E_{cell}: Cell potential

GC: Graphite Cathode

HRT: Hydraulic Residence Time

MEC: Microbial Electrochemical Cell

ORR: Oxygen Reduction Reaction

1. Introduction

1.1 Background

Hydrogen Peroxide (H_2O_2) is a strong oxidizing agent that is capable of oxidizing a wide variety of inorganic and organic substrates. H_2O_2 is also considered to be one of the most environmental-safe chemicals as H_2O and O_2 are only its reaction products. Thus, H_2O_2 is widely utilized in industrial applications, such as pulp and paper bleaching, textile industry, color-safe laundry bleaches (Campos-Martin, et al., 2006; Samanta, 2008). In addition, H_2O_2 plays a crucial role in advanced oxidation, tertiary wastewater treatment, and H_2S control in anaerobic digestion in water and wastewater treatment fields, (Andreozzi, et al., 1999; Campos-Martin, et al., 2006; Kepa, et al., 2008; Zhang, et al., 2008).

Conventionally, a multi-step H_2O_2 manufacturing process, known as *anthraquinone oxidation* (AO), is exclusively employed to meet the growing demand for H_2O_2; it currently accounts for approximately 95 % of the total H_2O_2 production. AO process enables the production of highly concentrated H_2O_2 (~ 70% H_2O_2 by weight). Despite its advantage of highly concentrated H_2O_2 production, AO process seems less sustainable due to high energy consumption. Also, there are additional costs associated with transport, storage, and handling of the H_2O_2 production process (Campos-Martin, et al., 2006). In a search for a more sustainable method for H_2O_2 production, a number of methods that apply the principle of generating H_2O_2 directly from H_2 and O_2 is underinvestigation: direct synthesis, photocatalysis, and fuel cell (Campos-Martin, et al., 2006; Samanta, 2008). The advantage of these methods is their ability to produce H_2O_2 with a minimal energy input at the location of its use, thereby eliminating the cost for transportation and handling. Recently, an emerging bio-technology called *Microbial Electrochemical Cell* (MEC) has exhibited

its potential as a sustainable alternative to the conventional H_2O_2 manufacturing process; the technology incorporates microbial metabolism into electrochemical generation of H_2O_2. Only a few studies showed H_2O_2 production in a lab-scale MEC (Rozendal, et al., 2009; Fu, et al., 2010[b]; Modin & Fukushi, 2012, Modin & Fukushi, 2013; Asghar, et al., 2014). Although the laboratory-scale studies proved the potential of MECs for H_2O_2 synthesis, they did not well-document the significance of several parameters that are directly related to the electrochemical generation of H_2O_2 in MECs. Therefore, this study was conducted to identify the relation between the parameters and the electrochemical generation of H_2O_2 in MECs. The study was then used to build and operate a pilot-scale MEC to assess the feasibility of the H_2O_2-producing MEC towards practical applications.

1.2 Microbial Electrochemical Cell (MEC)

An MEC is an emerging "green" technology that has been recognized for its two prime functions: 1) biological wastewater treatment and 2) value-added product (i.e. electric power, H_2, and H_2O_2). Due to its role for both wastewater treatment and value-added product recovery, the interest on MEC has surged in recent years with the ultimate goal of scaling up for water and wastewater treatment (Rabaey & Verstraete, 2005; Rozendal, et al., 2008; Logan & Rabaey, 2012).

Figure 1.1 illustrates a typical configuration of a dual-chamber MEC, typically designed for recovering value-added products in a cathode chamber. The dual-chamber MEC consists of the anode and the cathode compartment that are partitioned by a membrane. In MECs, a specific group of bacteria, so-called *anode-respiring bacteria* (ARB), are attached on the anode and they utilize biodegradable organic matters as a primary electron donor. During electrode-dependent

anaerobic respiration, electrons (e^-) and protons (H^+) are liberated from organics and transported to the cathode; the electrons travel to the cathode via an external electrical circuit, while the protons are transported through the membrane to the cathode for charge neutrality. Then, the electrons and protons react on the cathode to produce a value-added product. There are a wide variety of the value-added products that can be produced in MECs (i.e. electric power, H_2O_2, H_2, acetate, and so on) (Rabaey & Verstraete, 2005; Rozendal, et al., 2008; Logan & Rabaey, 2012). Although electric power generates spontaneously in MECs, an additional energy input to MECs would allow for the recovery of the value-added products that cannot be produced spontaneously, and can accelerate the production rate on electrodes (e.g., current). Consequently, retrofitting either a potentiostate or power supply to MECs is essential for synthesizing value-added products having higher energy status than organic fuels, such as H_2.

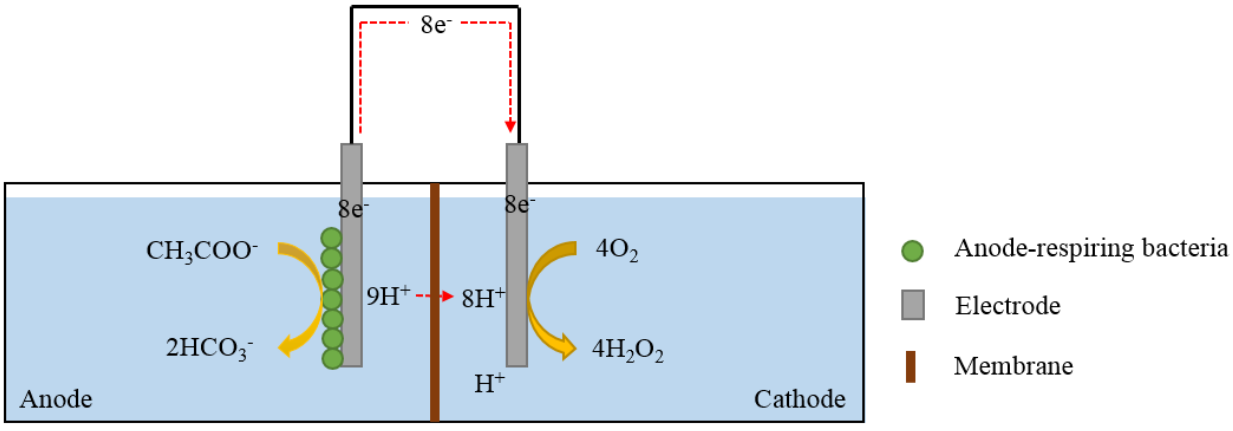

Figure 1.1: A typical configuration of a dual-chamber Microbial Electrochemical Cell.

1.2.1 Fundamental Electrochemistry in MECs

In electrochemical cells, redox reactions occur on two electrodes that are termed as an anode for oxidation reactions and a cathode for reduction reactions, and the overall reactions in

electrochemical cells can be evaluated with cell electromotive force (emf), E_{emf} (V) or cell potential. E_{emf} is the difference in potential between the anode and the cathode in an electrochemical cell and can be calculated using the following equation:

$$E_{emf} = E^{0}_{emf} - \frac{RT}{nF}\ln(II) \quad (1.1)$$

Where, E_{emf} is the cell electromotive force for a specific condition, E^{0}_{emf} is standard cell electromotive force under the standard conditions (standard condition: T = 298. 15 K, P = 1 atm, concentration for reactants and products = 1 M), R (8.31447 J mol_{-1} K^{-1}) is universal gas constant, *n* is the number of electrons per reaction mol, F (9.64853 X 10^4 C/mol) is Faraday's constant, and II is the reaction quotient (unitless) calculated as the activities of the products divided by the activities of the reactants. E_{emf} is used to evaluate whether or not the overall reaction within an electrochemical cell is thermodynamically favorable; a positive E_{emf} indicates a favourable reaction.

As E_{emf} is defined as the potential difference between the anode and the cathode ($E_{emf} = E_{cat} - E_{an}$), the electrode potential along with E_{emf} is also a variable of interest in electrochemical cells and is used to analyze the reactions taking place on electrodes. The following are the reactions with the corresponding standard potential at pH 7 in the MEC fed with acetate synthetic wastewater:

$$2HCO_3^- + 9H^+ + 8e^- \rightarrow CH_3COO^- + 4H_2O;\ E^o = -0.28\ V\ (vs\ NHE) \quad (1.2)$$

$$4H^+ + O_2 + 4e^- \rightarrow 2H_2O;\ E^o = +0.82V\ (vs\ NHE) \quad (1.3)$$

$$8H^+ + 4O_2 + 8e^- \rightarrow 4H_2O_2;\ E^o = +0.26\ V\ (vs\ NHE) \quad (1.4)$$

Reaction (1.2) is the oxidation reaction of the acetate on the anode while reaction (1.3) and (1.4) are the reduction reactions of oxygen (O_2) on the cathode for H_2O (water) and H_2O_2 (hydrogen peroxide) production, respectively. The standard potential for the above reactions is reported relative to a reference electrode known as the normal hydrogen electrode (NHE) that poises zero potential under the standard conditions. Practically, different reference electrodes can be used such as saturated calomel electrode (SCE) and silver chloride electrode (Ag/AgCl) reference electrode, which develop a potential difference of + 0.242 V and + 0.197 V against the NHE (Bard, et al., 2001).

With the standard potential, the theoretical potential for the electrodes can be calculated using the following equation, and eventually used to calculate the cell potential:

$$E_{electrode} = E^0_{electrode} - \frac{RT}{nF}\ln(II) \quad (1.5)$$

For example, the cell potential of the H_2O_2-producing MEC fed with the acetate synthetic wastewater can be calculated under the hypothetical conditions:

1. Acetate oxidation on anode: $[HCO_3^-]$ = 0.01 M, $[CH_3COO^-]$ = 0.025 M, and pH = 7

$$E_{anode} = E^0_{anode} - \frac{RT}{8F}\ln\left(\frac{[CH_3COO^-]}{[HCO_3^-]^2[H^+]^9}\right) = -0.296 \quad (1.6)$$

2. H_2O_2 formation on cathode: pO_2 = 0.2, $[H_2O_2]$ = 5 mM, and pH = 7

$$E_{cathode} = E^0_{cathode} - \frac{RT}{2F}\ln\left(\frac{[H_2O_2]}{pO_2[H^+]^2}\right) = +0.329 \quad (1.7)$$

3. Cell Potential:

$$E_{cell} = E_{cathode} - E_{anode} = 0.329 - (-0.296) = +0.625\ V \quad (1.8)$$

The theoretical cell potential for the H_2O_2-producing MEC fed with the acetate synthetic wastewater is calculated to be 0.625 V, implying that the reactions within the system are theoretically spontaneous. However, energy losses, which is termed as overpotential, always occur in an electrochemical cell (Bard, et al., 2001). Consequently, an external energy input with either a power supply or a potentiostate is often required to accelerate the desired reactions in an electrochemical cell.

1.2.2 H_2O_2-producing MEC

H_2O_2-synthesizing MECs share the same fundamentals for anodic reactions to conventional MECs, namely ARB metabolism. Hence, the characterization of cathodic reactions seems detrimental for the success of the MECs: improving O_2 reduction to H_2O_2 on the cathode, not H_2O. There have been a few studies conducted at a laboratory-scale MEC to demonstrate H_2O_2 production. Fu, et al (2010^a, 2010^b) produced H_2O_2 in MECs operated on synthetic wastewater without an additional energy input. Fu et al. demonstrated the H_2O_2 concentration of 78.85 mg/L after 12 hr-operation in the laboratory-scale system which was equipped with spectrographically pure graphite rods as the cathode (Fu, et al., 2010^b). Rozendal, et al (2009) also showed a high H_2O_2 production of 1.9 ± 0.2 kg H_2O_2/m^3/day in a MEC fed with the acetate synthetic wastewater at an expense of a low energy input of 0.5 V. Also, Modin & Fukushi, (2013) compared H_2O_2 production in a small system (with the liquid volume of 5 mL for the cathode compartment) when the system was operated on two feeds – 1) the acetate synthetic wastewater and 2) real wastewater-, and showed the significant lower H_2O_2 production when real wastewater was fed into the system. Literature only presents the proof-of-concept on H_2O_2 synthesis or its potential until now, although various

parameters on cathodic reactions (i.e. cathode potential, O_2 concentration, and cathode material) critically influence H_2O_2 yield and production rate in MECs. There is a need for characterizing cathodic reactions on the cathode to accelerate the success of H_2O_2-producing MECs.

1.3 Research Objectives

The research objectives were established to take a step-by-step approach with the eventual goal of building a pilot-scale MEC for the demonstration of H_2O_2 production; thus, the main objectives of this work were established as follows:

- Investigate the effect of cathode potential ($E_{cathode}$), cathode material, and aeration method on H_2O_2 production.
- Evaluate H_2O_2 production and wastewater treatment efficiency in a laboratory-scale MEC fed with acetate synthetic wastewater and domestic wastewater at different hydraulic residence times (HRTs) for the anode chamber.
- Investigate the feasibility of H_2O_2 production in a pilot-scale MEC fed with acetate synthetic wastewater.
- Identify the major operating challenges of a pilot-scale MEC.

1.4 Research Map

With the ultimate goal of operating a pilot-scale MEC for H_2O_2 production, the research was comprised of the three stages: 1) optimization of cathode operating conditions, 2) evaluation of the H_2O_2 production in a lab-scale MEC operated on acetate synthetic and domestic wastewater, and 3) H_2O_2 production in a pilot-scale MEC.

Initially, preliminary experiments were performed to establish optimal operating conditions ($E_{cathode}$, cathode material, and aeration method) for the cathode. The preliminary experiments solely depended on chemical reactions (such as water oxidation) and did not involve microbial metabolism to avoid damaging ARB during the preliminary experiments. Then, the laboratory-scale MEC was designed and constructed based on the results from the preliminary experiments, and operated under different operating conditions (such as feed and HRT) for H_2O_2 production. In the final stage of the research, a pilot-scale MEC was built and operated to demonstrate H_2O_2 production. Both laboratory-scale and pilot-scale MECs were evaluated based on COD removal efficiency, H_2O_2 production, and H_2O_2 yield efficiency.

1.5 Thesis Organization

The thesis is arranged in five chapters. In Chapter 1, a brief introduction on H_2O_2 and the need for a more sustainable method to produce H_2O_2 are addressed. Also, Chapter 1 provides fundamental knowledge in MECs and Electrochemistry, which are essential for understanding the system, and the objectives and the map of the research. In chapter 2-4, the experimental set-up, analytic methods, results, and the discussion of the three experiments are presented as follows: Chapter 2 (*Investigating the effect of cathodic parameters on the electrochemical generation of H_2O_2: cathode potential, cathode material, and aeration method*), Chapter 3 (*H_2O_2 production in a lab-scale MEC*), and Chapter 4 (*H_2O_2 production in a pilot-scale MEC*). Then, Chapter 5 summarizes the main findings from the research. Chapter 6 presents recommendations for further study on H_2O_2 production in MECs.

2. Investigating the effect of cathodic parameters on the electrochemical generation of H_2O_2: cathode potential, cathode material, and aeration method

Abstract

The electrochemical generation of hydrogen peroxide (H_2O_2) is possible via the oxygen reduction reactions (ORRs) that can be influenced by several variables, such as the cathode potential ($E_{cathode}$), cathode material, and aeration method. Thus, the study on the relation between those variables and H_2O_2 production via the ORRs was carried out to help establish the optimal operating conditions for the cathode of H_2O_2-producing microbial electrochemical cells (MECs). The study was divided in two phases. In the first phase, the graphite cathode (GC) and the carbon gas diffusion cathode (CGC) under active aeration were directly compared for H_2O_2 production and H_2O_2 conversion efficiency at the $E_{cathode}$ ranging from -0.4 V to -0.8 V (vs Ag/AgCl). In the second phase, the CGC was evaluated for H_2O_2 production at the $E_{cathode}$ of -0.4, -0.6, -0.8, -1.0, and -1.2 V (vs Ag/AgCl) when O_2 in the air was passively diffused to the cathode.

The direct comparison between the GC and the CGC under active aeration revealed that the CGC was better than GC for H_2O_2 production and H_2O_2 conversion efficiency for the range of $E_{cathode}$ from -0.4 to -0.8 V. However, the effect of $E_{cathode}$ on the electrochemical generation of H_2O_2 was profound for the cathodes under active aeration; O_2 reduction to H_2O was more favored as the $E_{cathode}$ became more negative. In the following phase, the H_2O_2 conversion efficiency improved substantially and the effect of the $E_{cathode}$ on H_2O_2 conversion efficiency diminished when O_2 in the air was passively diffused to the CGC; the H_2O_2 conversion efficiency ranging from 30 to 65 % at the $E_{cathode}$ ranging from -0.4 to -1.2 V.

2.1 Introduction

Electrochemical generation of H_2O_2 via the oxygen (O_2) reduction reactions (ORRs) has been introduced to supplant the highly energy-intensive AO process. Electrochemical generation of H_2O_2 has several advantages over the conventional AO process. The energy requirement for the emerging method is relatively low, and the on-site H_2O_2 production can lead to a significant reduction in cost for transportation, storage and handling (Campos-Martin, et al., 2006).

The ORRs follows three pathways: the direct O_2 reduction to H_2O, O_2 reduction to H_2O_2, and H_2O_2 reduction to H_2O whose standard potential at pH 7 is 0.82, 0.26, and 1.37 V (vs NHE), respectively. The ORR mechanisms are known to be complicated and influenced by a number of parameters. Among them, the cathode potential ($E_{cathode}$), cathode materials, and O_2 concentration have a direct impact on the ORRs (Song & Zhang, 2008). Therefore, the investigation on the effect of the parameters on the ORRs would be indispensable to maximize H_2O_2 formation via the ORRs.

The $E_{cathode}$ is a variable of significance, which would govern the reactions on the cathode. The optimal $E_{cathode}$ would be required to maximize O_2 reduction to H_2O_2 and minimize the side reactions, such as O_2 reduction to H_2O, H_2O_2 reduction to H_2O and H_2 evolution ($2H^+ + 2e^- \rightarrow H_2$; E^o = -0.4 at pH 7). Yamanaka & Murayama, (2008) compared H_2O_2 formation rate and H_2O_2 conversion efficiency (the ratio of electrons converted to H_2O_2 to the total electrons produced) in the range of the $E_{cathode}$ from 0 to -0.4 V (vs Ag/AgCl), and observed the maximum H_2O_2 formation rate and H_2O_2 conversion at the $E_{cathode}$ of -0.3 V (vs Ag/AgCl). He also reported that H_2 conversion efficiency was increased from 6.8 to 23.4 % when the $E_{cathode}$ was decreased from -0.3 V to -0.4 V (vs Ag/AgCl). Similarly, Qiang, et al (2002) observed that H_2O_2 reduction to H_2O and H_2 evolution were favored when the $E_{cathode}$ was decreased beyond -0.5 V (vs SCE) in acidic

solution. Based on the results from the past studies, the $E_{cathode}$ in that range would rather favor the cathodic reactions of O_2 reduction to H_2O, H_2O_2 reduction to H_2O, and H_2 formation, adversely affecting the electrochemical generation of H_2O_2. Therefore, it is important to confirm the effect of the $E_{cathode}$ within the range on H_2O_2 production via the ORRs.

The cathode material also plays a key role in ORRs. Graphite and carbon gas diffusion electrode are the cathode materials mainly used in many studies which focused on the electrochemical generation of H_2O_2 (Qiang, et al., 2000; Brillas, et al., 2002; Pozzo, et al., 2005; Agladze, et al., 2006; Panizza & Cerisola, 2008; Yamanaka, 2008; Yamanaka & Murayama, 2008; Reis, et al., 2011). Pozzo, et al (2005) performed the comparison of two cathode materials - a graphite electrode and a gas diffusion electrode - in two different cells for H_2O_2 production, and showed higher H_2O_2 production with the latter material. However, it is noted that a different aeration method was implemented for each cathode material, making it difficult to directly compare the cathode materials for the electrochemical generation of H_2O_2; the graphite electrode was actively aerated while the gas diffusion electrode was passively aerated. The use of the gas diffusion electrode would not need aeration, which could substantially decrease the operating cost at a large-scale system. However, Qiang, et al (2002) exploited the graphite plate as the cathode, and produced H_2O_2 concentration of 80 mg/L in 2 hours, proving the applicability of the graphite plate for the electrochemical generation of H_2O_2. Therefore, the direct comparison between the graphite cathode and the gas diffusion electrode under the equivalent operating conditions would be required to determine the cathode material that is more suitable for the electrochemical generation of H_2O_2.

In addition, O_2 concentration is a key feature in ORRs. A number of past studies illustrated that H_2O_2 production improved as O_2 concentration was increased (Brillas, et al., 2002; Qiang, et al., 2002). Qiang, et al (2002) compared H_2O_2 production when pure oxygen gas (99.6 %) (Equilibrium dissolved oxygen concentration: 39.3 mg/L at pH 2) and air (Equilibrium dissolved oxygen concentration: 8.3 mg/L at pH 2) were sparged to supply oxygen, and showed that H_2O_2 production was higher with the pure oxygen gas. Also, Brillas, et al (2002) passively aerated the gas diffusion electrode at different oxygen partial pressures (from 0.21 to 1.00 atm) and found the highest H_2O_2 production with the highest oxygen partial pressure of 1.00 atm. These studies indicated that H_2O_2 production correlates with oxygen concentration. However, no comparative study between the active aeration and the passive aeration has been conducted to examine its effect on the electrochemical generation of H_2O_2.

The previous studies clearly suggested the profound effect of $E_{cathode}$, cathode material, and O_2 concentration on the electrochemical generation of H_2O_2 via the ORRs; therefore, the thorough evaluation of those parameters on H_2O_2 production is required and it would be a sound foundation for the optimal H_2O_2 production from MECs. Consequently, the preliminary experiments were conducted in two phases to examine the effect of those parameters on H_2O_2 formation. In phase I, the graphite cathode (GC) and the carbon gas diffusion cathode (CGC) under direct aeration were evaluated for H_2O_2 production at a range of the $E_{cathode}$ from -0.4 to -0.8 V. In the following phase (phase II), the CGC was evaluated for H_2O_2 production under the passive air diffusion at a range of the $E_{cathode}$, and this would allow the comparison of H_2O_2 production for the CGC under a different aeration method.

2.2 Materials & Methods

2.2.1 Reactor Configuration

An electrochemical cell was constructed in the engineering machine shop in the University of Waterloo for the preliminary experiments (Figure 2.1).

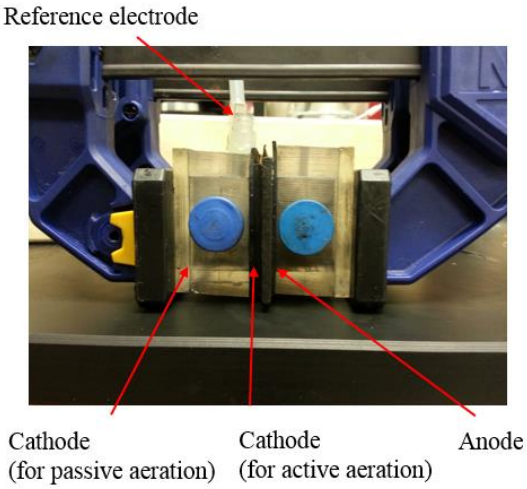

Figure 2.1: An electrochemical cell built for the preliminary experiments.

It consists of an anode chamber, a cathode chamber, two electrodes (an anode and a cathode), and a membrane. The dimensions of the anode chamber and cathode chamber for the cell were 3.5 cm×5 cm×2.5 cm; the working volumes of the anode and cathode chambers were 35 and 25 mL. Due to the intensive mixing for the direct aeration in the cathode, the working volume for the cathode chamber was reduced to 25 mL. A graphite plate (Isomolded Graphite Plate 203101, Fuel Cell Earth) was used as the anode with the projected surface area of 17.4 cm^2. For the cathode, two cathode materials with the projected surface area of 17.4 cm^2 were used over the course of the preliminary experiments: a graphite cathode (GC) (Isomolded Graphite Plate 203101, Fuel Cell Earth) and a carbon gas diffusion cathode (CGC) (GDS2230, Fuel Cell Earth). Cation exchange membrane (CEM) (CMI-7000, Membranes International Inc., USA) with the projected surface

area of 17.4 cm^2 was used as the membrane in the electrochemical cell. The CEM was selected as the membrane as it would allow the protons (H^+) to travel from the anode the cathode and to eventually react with electrons (e^-) and O_2 to form H_2O_2. To control the $E_{cathode}$ with a potentiostat (BioLogic, VSP, Gamble Technologies, Canada), an Ag/AgCl reference electrode (MF-2052, Bioanalytical System Inc. (BASI), USA) was located ~0.5 cm apart from the cathode in the cathode chamber. Hereinafter, the $E_{cathode}$ is reported relative to the Ag/AgCl reference electrode in Chapter 2.

2.2.2 Operating Conditions

For each experimental run in the preliminary experiments, the anode and cathode chamber of the electrochemical cell were filled with de-ionized water (18 MΩ-cm). A magnetic stirrer was also inserted into each chamber to establish the intense mixing condition, thereby minimizing the mass transfer limitation. The cell was operated in two different aeration modes: direct aeration (Phase I) and passive diffusion (Phase II). In phase I, an air blower (DW-12, Tetron Product, Taiwan) was used to directly aerate the cathode chamber at a flow rate of 860 mL/min for the GC and the CGC. In Phase II, O_2 was passively diffused to the CGC cathode. Consequently, the cathode was placed on the end of the cathode chamber for its direct exposure to the air, creating 2-cm spacing between the cathode and the anode (see Figure 2). In phase I and phase II, $E_{cathode}$ was varied to examine the effect of the $E_{cathode}$ on H_2O_2 production using the potentiostat. The $E_{cathode}$ was varied from -0.4 to -0.8 V and from -0.4 to -1.2 V by an increment of -0.2 V for phase I and phase II, respectively. For both phases, the electrochemical cell was operated in batch mode for 180 mins, and 0.5 mL sample was collected from the cathode chamber every 30 min for H_2O_2 quantification.

To evaluate the performance of the cell for each experimental run, electrode potentials and current were monitored throughout each 180-min operation using EC-Lab software in a personal computer connected to the potentiostat.

2.2.3 Analytical methods and Computation

The vandate method was employed for H_2O_2 quantification (Nogueira et.al, 2005). For this method, the vandate solution in which the concentration of vandate and sulfuric acid was 0.06 and 0.28 M, respectively, was prepared. To measure H_2O_2 concentration, 0.5 mL of the vandate solution and 0.5 mL of sample were added to a Hach vial and diluted to 5 mL with de-ionized water. Using Hach spectrophotometer, H_2O_2 was measured at the wavelength of 450 nm. The calibration curve for the vandate method was made using 8 standards with various H_2O_2 concentrations ranging from 0 mg/L to 1500 mg/L. H_2O_2 concentration was normalized with the surface area of the cathode (17.4 cm^2). Based on measured H_2O_2 concentration and cumulative coulombs in a given time, the conversion efficiency of coulombs to H_2O_2 was calculated using the following equation.

$$H_2O_2 \text{ Conversion Efficiency } (\%) = \frac{nFC_{H_2O_2}V}{\int_0^t I\,dt} \times 100 \qquad (2.1)$$

Where n = mole of electrons equivalent to mole of H_2O_2 (n=2)

F = the Faraday constant (96,500 C/mol)

C_{H2O2} = the measured H_2O_2 concentration (mol/L)

V = the catholyte volume (L)

The current was monitored and recorded using EC-Lab. The current was normalized with the surface area of the membrane (17.4 cm^2) and was reported as the current density.

2.3 Results & Discussion

2.3.1 Graphite Cathode vs Carbon Gas Diffusion Cathode under Active Aeration

Figure 2.2 presents the average current density and the cell voltage at the $E_{cathode}$ of -0.4, -0.6 and -0.8 V for the GC and CGC as the cathode. The current densities and the cell voltages for both cathodes increased as the $E_{cathode}$ became more negative. However, the GC resulted in the higher current densities and the cell voltage than the CGC for the range of the $E_{cathode}$. The current densities (cell voltages) for the GC were 1.40 ± 0.40 (2.11 ± 0.04 V), 66.85 ± 5.00 (4.20 ± 0.11 V) and 71.20 ± 8.90 A/m^2 (4.26 ± 0.20 V) at the $E_{cathode}$ of -0.4, -0.6, and -0.8 V, respectively. On the other hand, the current densities (cell voltages) for the CGC were 3.47 ± 0.92 (1.80 ± 0.01 V), 17.63 ± 1.09 (2.38 ± 0.07 V), and 42.59 ± 4.06 A/m^2 (2.95 ± 0.13 V) at the $E_{cathode}$ of -0.4, -0.6, and -0.8 V, respectively.

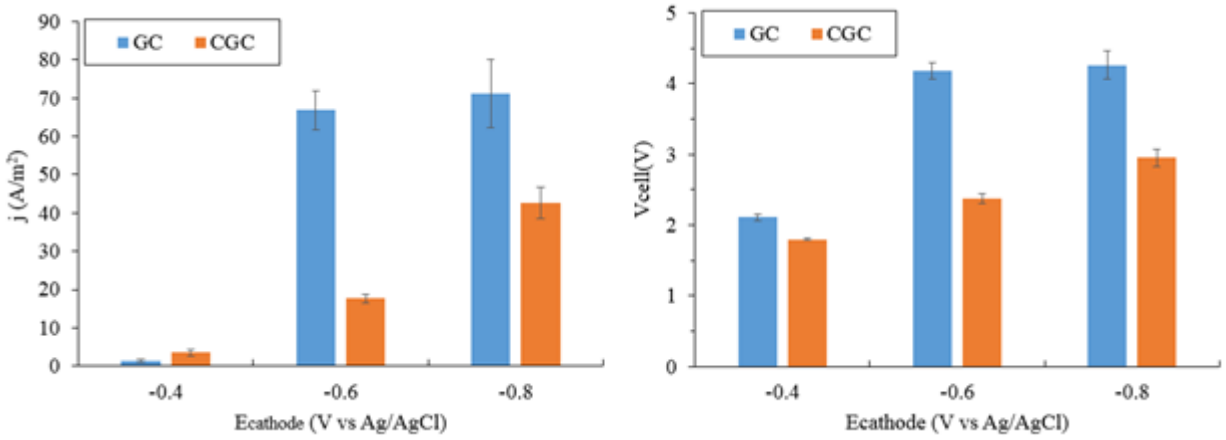

Figure 2.2: Average current density (left) and cell voltage (right) for both cathodes in phase I. (bars represent standard deviation)

Figure 2.3 shows cumulative H_2O_2 concentration in the cathode chamber over the course of 180-min operation for each $E_{cathode}$. It is apparent that the $E_{cathode}$ played a key role on H_2O_2 production via the ORRs. Each cathode showed the difference of the H_2O_2 production rate against $E_{cathode}$ (more details in Figure 2.3). Figure 2.3 indicated the faster H_2O_2 production rate with the CGC than that with the GC, although the higher current densities were observed with the GC than the CGC (Figure 2.2). The highest cumulative H_2O_2 concentration at the end of the 180-min operation was 17.54 mg·L^{-1}·cm^{-2} (at the $E_{cathode}$ of -0.6 V) and 1.77 mg·L^{-1}·cm^{-2} (at the $E_{cathode}$ of -0.8 V) for the CGC and the GC, respectively.

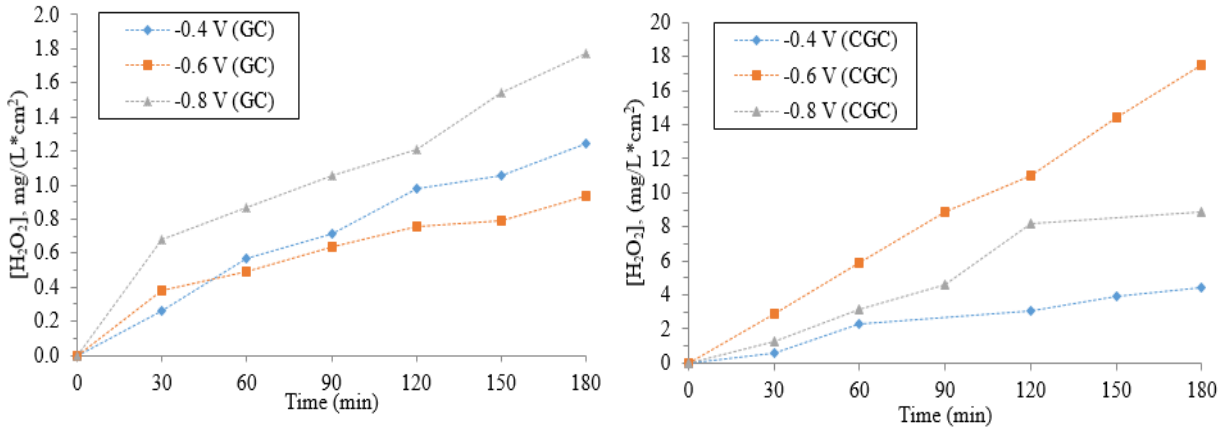

Figure 2.3: Cumulative H_2O_2 concentration in 180-min operation in phase I for GC (left) and CGC (right).

Figure 2.4 presents the H_2O_2 conversion efficiency for both cathodes at different $E_{cathode}$. It shows that H_2O_2 conversion efficiency with the CGC were relatively higher than those with the GC. With the GC, the H_2O_2 conversion efficiency at the $E_{cathode}$ of -0.4, -0.6 and -0.8 V was 12, 0.2, and 0.3 %, respectively. In contrary, the CGC had the H_2O_2 conversion efficiency of 16, 12 and 2.5 % at the $E_{cathode}$ of -0.4, -0.6 and -0.8 V, respectively. This indicated that the CGC favored the O_2 reduction to H_2O_2 more than the GC. Figure 2.4 also pointed out that the $E_{cathode}$ had a direct impact

on H_2O_2 production via the ORRs when the cathode was actively aerated. As the $E_{cathode}$ became more negative, O_2 reduction to H_2O was more favored.

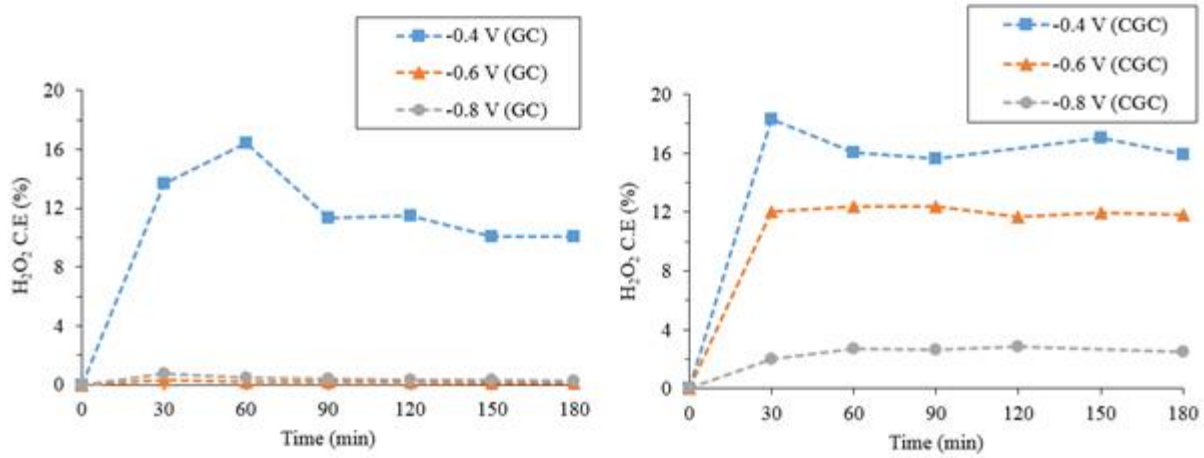

Figure 2.4: H_2O_2 conversion efficiency over 180-min operation for GC (left) and CGC (right) in phase I.

2.3.2 Carbon Gas Diffusion Cathode under Passive Air Diffusion

Figure 2.5 presents the average current density and the cell voltage for the CGC under the passive diffusion. In agreement with the trend in the current density and the cell voltage from phase I, the current density and the cell voltage in this phase was also increased as the $E_{cathode}$ was more negative. However, the lower current density and the higher cell voltage in phase II was observed than those in phase I with the CGC at an equivalent $E_{cathode}$ (Figure 2.2); the current density (cell voltage) in phase II was 0.06 ± 0.01 (1.41 ± 0.03 V), 0.34 ± 0.03 (1.93 ± 0.03 V), 1.10 ± 0.06 (3.29 ± 0.06 V), 1.32 ± 0.13 (4.51 ± 0.13V), 6.71 ± 1.36 A/m^2 (4.67 ± 0.40V) at the $E_{cathode}$ of -0.4, -0.6, -0.8, -1.0, and -1.2 V, respectively. This result indicates that mass transport of O_2 mainly limits current in the electrochemical cell equipped with the CGC under air diffusion conditions.

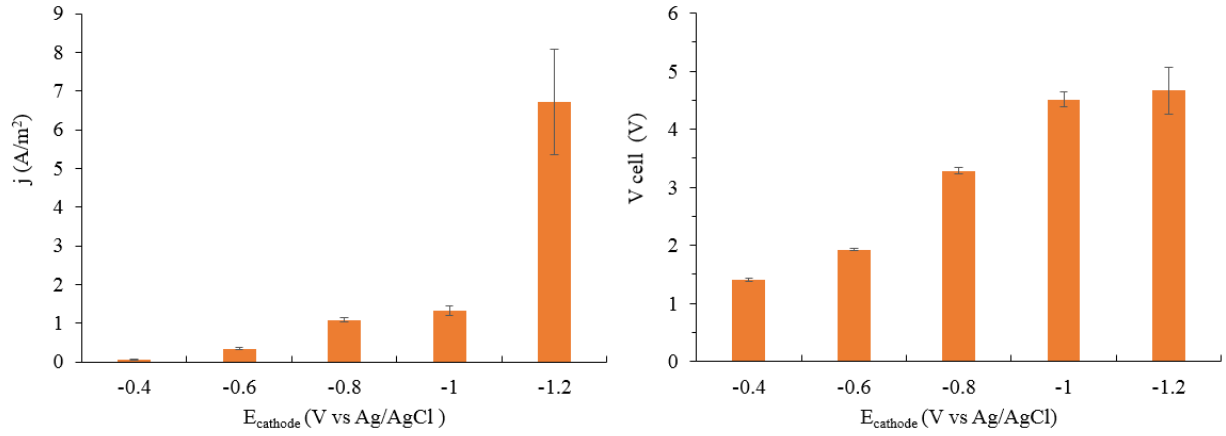

Figure 2.5: Average current density (left) and the cell voltage (right) in phase II (bars represent standard deviation).

Figure 2.6 displays cumulative H_2O_2 concentration over 180-min operation for the range of the $E_{cathode}$ from -0.4 to -1.2 V. It was apparent that H_2O_2 production was linearly correlated to the $E_{cathode}$. The highest cumulative H_2O_2 of 5.99 $mg \cdot L^{-1} \cdot cm^{-2}$ was observed at the $E_{cathode}$ of -1.2 V while the lowest cumulative H_2O_2 of 0.16 $mg \cdot L^{-1} \cdot cm^{-2}$ was found at the $E_{cathode}$ of -0.4 V.

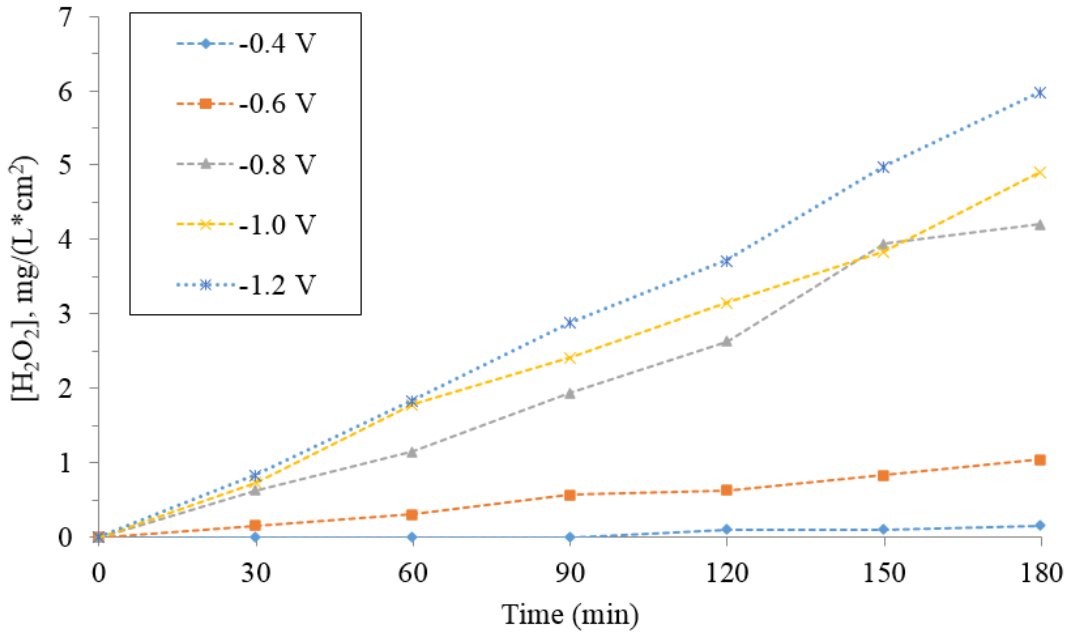

Figure 2.6: Cumulative H_2O_2 concentration in 180-min operation in phase II.

Figure 2.7 illustrates the H_2O_2 conversion efficiency evolution in 180-min operation within the range of the $E_{cathode}$ from -0.4 to -1.2 V. The H_2O_2 conversion efficiency was relatively consistent after the first 30 min until the end for each experiment. This result reveals that the passive O_2 diffusion to the cathode improves the H_2O_2 conversion efficiency. The H_2O_2 conversion efficiency ranged from the minimum H_2O_2 conversion efficiency of 30 % (at the $E_{cathode}$ of -0.4 V) to the maximum H_2O_2 conversion efficiency of 65 % (at the $E_{cathode}$ of -0.6, -0.8, -1.0, and -1.2 V). Further study is required to find any fundamental reasons for this abnormal phenomenon; however, low current density, high O_2 concentration (43 mM in gas phase vs. 1.8 mM in liquid phase at 1 atm and 281 K), and mass transport limitation would favor the electrochemical formation of H_2O_2.

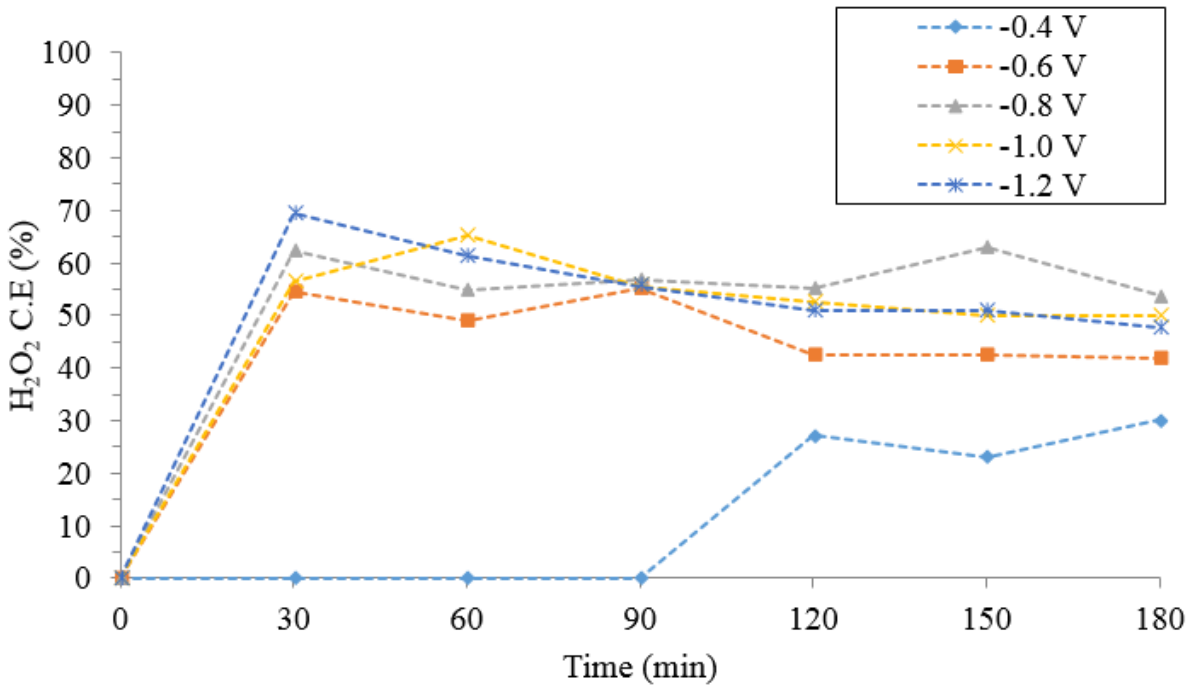

Figure 2.7: H_2O_2 conversion efficiency evolution in 180-min in phase II.

2.4 Conclusions

Oxygen reduction reactions (ORRs) involve complicated mechanisms, which are dictated by cathode material, $E_{cathode}$, and aeration method. As a result, the parameters have a direct impact on the electrochemical generation of H_2O_2 via the ORRs. In the preliminary experiments, the effect of cathode material, $E_{cathode}$, and aeration method on ORRs was examined.

The first set of the preliminary experiments compared the GC and the CGC for H_2O_2 production for a range of $E_{cathode}$ from -0.4 to -0.8 V when the active aeration was implemented for the cathodes. Higher current densities were observed with the GC for the range of the $E_{cathode}$; the maximum current density was 71.20 ± 8.90 and 42.59 ± 4.06 A/m^2 for the GC and the CGC, respectively, at the $E_{cathode}$ of -0.8 V. However, the CGC resulted in higher H_2O_2 production rate than the GC; the

highest H_2O_2 production rate for the CGC and the GC was 1.77 $mg \cdot L^{-1} \cdot cm^{-2}$ (at the $E_{cathode}$ of -0.6 V) and 17.54 $mg \cdot L^{-1} \cdot cm^{-2}$ (at the $E_{cathode}$ of -0.8 V). These results imply that the CGC and the GC favored O_2 reduction to H_2O_2 and H_2O, respectively. Nonetheless, the H_2O_2 conversion efficiency was low for both cathodes; the highest H_2O_2 conversion efficiency was 12 % and 16 % for the GC and the CG, respectively, at the $E_{cathode}$ of -0.4 V. These results indicate that O_2 reduction to H_2O was dominant for both cathodes under the operating conditions.

In the second set of the experiments, H_2O_2 production was evaluated when O_2 in the air was passively diffused to the CGC for a range of the $E_{cathode}$ from -0.4 to -1.2 V. For the range of the $E_{cathode}$, the current density ranged from 0.06 ± 0.01 to 6.71 ± 1.36 A/m^2. The maximum H_2O_2 production rate was 5.99 $mg \cdot L^{-1} \cdot cm^{-2}$ at the $E_{cathode}$ of -1.2 V. However, the passive air diffusion improved O_2 reduction to H_2O_2 significantly, as indicated with the H_2O_2 conversion efficiency ranging from 30 % to 65 %. Passive air diffusion induced low current density, high O_2 concentration and O_2 mass transportation limitation under which the electrochemical generation of O_2 via the ORRs was favored.

3. H_2O_2 Production in a Laboratory-scale Microbial Electrochemical Cell

Abstract

With the growing concern with the conventional H_2O_2 manufacturing process due to its high energy consumption, MEC has emerged as the sustainable alternative for the production of H_2O_2. In this study, a laboratory-scale MEC was operated and evaluated for H_2O_2 production under various operating conditions, such as feed (synthetic acetate wastewater vs real wastewater) and HRT.

When the laboratory-scale system was operated with the acetate synthetic wastewater as the feed (acetate-fed MEC), the acetate in the synthetic wastewater was efficiently degraded by ARB at the range of the HRT from 2 to 24 hrs; the COD removal efficiency ranged from 45 ± 2 to 94 ± 2 % and the coulombic efficiency ranged from 37 ± 2 to 82 ± 2 %. As a result, the acetate-fed MEC showed high current density, which ranged from 2.9 ± 0.27 to 8.0 ± 0.59 A/m^2 in the range of the HRT from 24 hrs to 2 hrs, respectively. This led to high H_2O_2 production with the minimum and maximum cumulative H_2O_2 concentration of 285.56 ± 16.17 mg/L and 843.49 ± 17.29 mg/L in 6 hrs of cathode operation at the HRT of 24 and 2 hrs, respectively. At 6 hrs of cathode operation, the H_2O_2 conversion efficiency ranged from 36.15 ± 0.39 to 48.53 ± 0.10 % for the range of the HRTs. However, the high pH (pH>8) and the accumulation of H_2O_2 with time in the cathode triggered both H_2O_2 self-decomposition and H_2O_2 reduction to H_2O, reducing the H_2O_2 conversion efficiency at 24 hr of cathode operation, which ranged from 17.21 ± 0.31 to 29.35 ± 0.50 %. In the wastewater-fed MEC, the COD in domestic wastewater was efficiently degraded; the COD removal efficiency ranged from 39 ± 7 to 64 ± 5 % within the range of the HRTs from 2 to 10 hrs, respectively. However, non-ARB consumed the majority of the substrates in the wastewater,

leading to substantially low current density and H_2O_2 production; the current density ranged from 0.28 ± 0.05 (at the HRT of 10 hrs) to 0.56 ± 0.05 A/m^2 (at the HRT of 6 hrs) and the cumulative H_2O_2 concentration at the end of 24 hr-operation ranged from 37.59 ± 1.98 (at the HRT of 2 hrs) to 147.73 ± 1.98 mg/L (at the HRT of 6 hrs).

The findings from the laboratory-scale MEC demonstrated the possibility of the MEC as a sustainable method to manufacture H_2O_2. Also, HRT is an operating parameter of significance in order to achieve a targeted H_2O_2 concentration. However, this study highlights the need for the future study to improve current generation and H_2O_2 production in wastewater-fed MECs.

3.1 Introduction

Microbial Electrochemical Cell (MEC) has emerged as a sustainable technology for its ability to concurrently treat wastewater and produce value-added products (i.e. electric power, H_2, and H_2O_2). In the recent years, the recovery of the various value-added products in lab-scale MECs has been well-documented in a number of the studies (Escapa, et al., 2014; Pikaar, et al., 2014; Zhang & Angelidaki, 2014). Among the wide variety of the value-added products, H_2O_2 has drawn the attention of the research communities mainly due to growing concerns related to the conventional H_2O_2 manufacturing process, known as *anthraquinone oxidation* (AO) process. Currently, the AO process is world-widely used to meet the surging demand for the chemical, accounting for approximately 95 % of the global production of H_2O_2 (Campos-Marin, et al., 2006). The research for a sustainable alternative to replace the AO process is on-going due to considerably high energy consumption and other additional costs (i.e. transportation, storage, and handling) associated with the AO process. In this regard, H_2O_2-producing MECs pose a promising potential as the sustainable H_2O_2 manufacturing method. MECs exploit microbial metabolism for biological wastewater treatment under anaerobic conditions. Due to no requirement for the aeration that is accountable for high energy consumption in conventional wastewater treatment facilities, the substantial reduction in the operation costs for MECs would be possible (Goldstein, 2002). In addition, the MEC can be constructed at the location of the use for the chemical and this would further reduce the costs for the transportation, storage and handling.

In the MECs for H_2O_2 production, the redox reactions - the oxidation of biodegradable contaminants (i.e. acetate) in the anode and the reduction of O_2 to H_2O_2 in the cathode - occur. The following are the redox reactions with its corresponding standard potential at pH 7 in the MEC fed with acetate (CH_3COO^-) synthetic wastewater for H_2O_2 production via ORRs:

1. Oxidation reaction of CH_3COO^- in the anode:

$$2HCO_3^- + 9H^+ + 8e^- \rightarrow CH_3COO^- + 4H_2O;\ E^o = -0.28\ V\ (vs\ NHE) \quad (3.1)$$

2. Reduction reaction of O_2 to H_2O_2 in the cathode:

$$8H^+ + 4O_2 + 8e^- \rightarrow 4H_2O_2;\ E^o = +0.26\ V\ (vs\ NHE) \quad (3.2)$$

Under the standard conditions (T = 298 K, 1 atm, 1 M), E_{emf} is calculated to be 0.54 V. The positive E_{emf} of 0.54 V under the standard conditions indicates that the overall reaction is thermodynamically favorable, meaning that MECs does not require an energy input for H_2O_2 generation. Fu, et al (2010)[a] showed H_2O_2 production in the MEC with an external resistance of 20 Ω connected between the anode and the cathode, attaining the cumulative H_2O_2 concentration of 78.85 mg/L in a 12-hr operation. Furthermore, Feng, et al (2010) and Fu, et al (2010)[b] proposed a "*Bio-Electron-Fenton*" process, which involves H_2O_2 and ferrous iron (Fe^{2+}) generated via the cathodic reactions in MECs. Using the bio-electron-fenton process, they demonstrated the efficient treatment of biorefractory organic substances, such as Orange II and azo dyes. Although these studies exhibited the possibility of H_2O_2-producing MECs without an energy input, several studies showed that H_2O_2 production in MECs improved considerably with an external energy input (Rozendal, et al, 2009; Modin & Fukushi, 2012, Modin & Fukushi, 2013). Modin & Fukushi, (2012) reported an increase in H_2O_2 production with an energy input. In the MEC with no energy input, the cumulative H_2O_2 concentration of 809.1 mg/L was achieved in 72.1 hrs of the operation. However, the cumulative H_2O_2 concentration of 4588.8 mg/L in 21 hrs of the operation was reported in the identical system when the anode potential was controlled at -0.11 V (vs NHE), resulting in the energy use of 1.77 kWh/kg H_2O_2. Also, Rozendal, et al (2009) demonstrated the production of ~1.9 ± 0.2 kg H_2O_2/m^3/day when the voltage of 0.5 V was applied to the MEC.

In this chapter, the applicability of the MEC technology for H_2O_2 production was assessed at a laboratory scale. The effect of the HRT and the feed on the performance of the lab-scale H_2O_2-producing MEC was investigated and their implications in terms of the applicability of the H_2O_2-producing MEC were discussed.

3.2 Material & Method

3.2.1 Reactor Configuration

Figure 3.1 shows the lab-scale MEC used to assess the applicability of the MEC technology as the sustainable method to manufacture H_2O_2. The MEC was fabricated with cylindrical plexiglass and had a dual-chamber configuration; it consisted of an anode (inner diameter: 3.2 cm and length: 8 cm) and a cathode chamber (inner diameter: 3.2 cm and length: 2 cm) whose working volume was 289 mL and 70 mL, respectively.

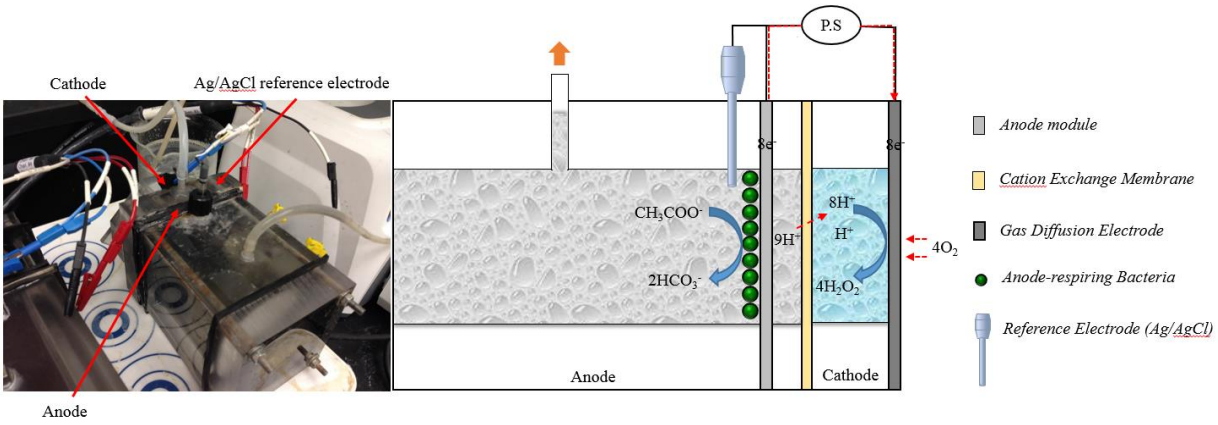

Figure 3.1: Picture (left) and the schematic diagram (right) of the lab-scale MEC.

To increase ARB biofilm density that would directly impact the current generation, an anode module was designed to increase the surface area of the anode and incorporated into the anode

chamber of the MEC (Figure 3.2). For the anode module, high density carbon fibers (2293-A, 24A Carbon Fiber, Fibre Glast Development Corp., Ohio, USA) was connected with a stainless steel frame. The carbon fibers were pretreated for the enhancement of the ARB attachment onto the anode by immersing in nitric acid (1 N), acetone (1 N), and ethanol (1 N) each for 1 day in sequence, and washed thoroughly with de-ionized water.

Figure 3.2: An anode module incorporated into the lab-scale MEC

The carbon gas diffusion cathode (CGC) (GD2230, Fuel Cell Earth, USA) with the projected surface area of 33 cm^2 was selected as the cathode because the preliminary experiments indicated that the CGC was a suitable cathode material for H_2O_2 production via ORRs. The cathode was located ~ 2.5 cm apart from the anode for the direct exposure to the air; the implementation of the passive aeration for the cathode was taken into the consideration for the design of the MEC.

The CEM (CMI-7000, Membranes International Inc., USA) with the surface area of 33 cm^2 was selected as the membrane because the CEM would allow protons (H^+) to travel from the anode to the cathode to form H_2O_2. An Ag/AgCl reference electrode (MF-2052, Bioanalytical System Inc. (BASI), USA) was placed ~0.5 cm apart from the anode module in the anode chamber to control

the anode potential (E_{anode}). To control the E_{anode}, a potentiostat (BioLogic, VSP, Gamble Technologies, Canada) was connected to the reference electrode.

3.2.2 Inoculation and Start-up

Prior to the experiments, the anode-respiring bacteria (ARB) acclimation was carried out for ~ 2 weeks until the steady-state current density was achieved. The anode chamber of the lab-scale MEC was inoculated with 10 mL of the effluent from an existing MEC at Waterloo Environmental Biotechnology (WEB) laboratory and acetate synthetic wastewater (25 mM sodium acetate). The composition of the synthetic wastewater was (per L of 18.2 MΩ cm MilliQ water) 2050 mg/L CH_3COONa, 2274 mg KH_2PO_4, 11,678 mg $Na_2HPO_4 \cdot 12H_2O$, 37 mg NH_4Cl, 25 mg $MgCl_2 \cdot 6H_2O$, 6 mg $MnCl_2 \cdot 4H_2O$, 0.1 mg $CuSO_4 \cdot 5H_2O$, 0.1 mg $Na_2WO_4 \cdot 2H_2O$, 0.1 mg $NaHSeO_3$, 0.01 mg $CaCl_2 \cdot 2H_2O$, 0.5 mg $ZnCl_2$, 0.1 mg $AlK(SO_4)_2$, 0.1 mg H_3BO_3, 0.1 mg $Na_2MoO_4 \cdot 2H_2O$, 0.2 mg $NiCl_2$, 5 mg EDTA, 1 mg $CO(NO_3)_2.6H_2O$, and 0.2 mg $NiCl_2 \cdot 6H_2O$. The medium was autoclaved and sparged with ultra-pure nitrogen (99.999%) for 30 min. Then, $FeCl_2 \cdot 2H_2O$ (20 mM) and $Na_2S \cdot 9H_2O$ (77 mM) were added to the medium (1 mL per L). Medium pH was constant at 7.3 ± 0.1. The cathode chamber was filled with de-ionized water (18.2 MΩ cm). Both the anode and the cathode chambers were operated in a batch mode until the steady-state current density of ~ 8.0 A/m^2 was achieved. During the ARB acclimation, the anode potential (E_{anode}) was fixed at -0.4 V (vs Ag/AgCl) to optimize the ARB biofilm formation.

3.2.3 Operation

When the steady-state current density of 8.0 A/m^2 was achieved during the ARB acclimation, the operation for the MEC experiments commenced. For the MEC experiments, the operation for the anode chamber was switched from the batch to the continuous mode using a peristaltic pump (Masterflex, Model 7523-80, USA), while the batch mode was maintained for the cathode chamber. Two phases were carried out in the lab-scale MEC experiments. In the first phase, acetate synthetic wastewater (5 mM sodium acetate) was fed into the anode chamber (acetate-fed MEC) at a different hydraulic residence time (HRT) of 24, 10, 8, 6, 4, and 2 hrs. The rationale for feeding the acetate synthetic wastewater (5mM sodium acetate) is the COD concentration equivalent to 320 mg/L that is in the range of the COD concentration for typical municipal wastewater (Metclf, et al., 2004). In the second phase, raw wastewater collected from Waterloo Municipal Wastewater Treatment Plant (Waterloo, Ontario, Canada) was fed to the anode chamber (wastewater-fed MEC) at the HRT of 10, 6, and 2 hrs. When the steady-state current density was reached for each HRT, the cathode chamber was rinsed with de-ionized water three times, and filled with fresh de-ionized water for the experiments. For the experiments, the cathode chamber was operated in a batch mode for 24 hrs, and the sample was collected from the cathode chamber for H_2O_2 quantification. Also, the effluent samples were collected from the anode chamber for the chemical oxygen demand (COD) analysis. For H_2O_2 quantification and COD analysis, the samples were collected and measured in triplicate. In addition, the current, electrode potentials, and cell voltage were monitored via EC-Lab for windows v10.12 software in a personal computer connected with the potentiostat.

3.2.4 Analytical method and Computation

H_2O_2 quantification was carried out using the vandate method (Nogueira, et al., 2005), and H_2O_2 conversion efficiency was calculated based on measured H_2O_2 concentration. The method for quantifying H_2O_2 and calculating H_2O_2 conversion efficiency is presented in Chapter 2.2.3

Chemical oxygen demand (COD) concentrations were analyzed colorimetrically according to method 5220 D of the Standard Methods. For COD concentration measurement, samples were digested in a preheated HACH COD reactor at 150 ℃ for 2 hours before the absorbance measurements were carried out with a UV spectrophotometer (DR/ 2000, HACH Company, USA) at a wavelength of 600 nm.

COD removal efficiency (R_t) was expressed:

$$R_t = \frac{COD_{inf} - COD_{eff}}{COD_{inf}} \times 100\% \quad (3.3)$$

Where, COD_{inf}, and COD_{eff} are the TCOD of the influent and the effluent, respectively.

Based on the COD removal and cumulative coulombs, coulombic efficiency was calculated with equation (3.5); the coulombic efficiency represents the ratio of the electrons transferred to the anode by ARB to the electrons released from electron donor (feed).

$$\text{Coulombic efficiency} = \frac{MI}{Fbq\Delta COD} \quad (3.4)$$

Where, M (=32 g/mol) is molecular weight of oxygen, *I* is the current (in A), F (=96495 A·s/mol) is Faraday's constant, b (=4 mol) is the number of electrons exchanged per mole of oxygen, q is the volumetric influent flow rate, and ΔCOD is the difference in the influent and the effluent COD.

In order to determine if the experimental results for the measurements were significantly different, the Student's t-test was used to test the hypothesis of quality at a 95 % confidence level.

$$\text{One sample t} - \text{test} = \frac{\bar{x}-\mu_0}{s/\sqrt{n}} \quad (3.5)$$

Where,

$\bar{x}$ = Sample mean

s = Sample standard deviation

n = Sample size

The null hypothesis was defined to be no difference between measurements while the alternative hypothesis was defined that there is a statistical difference between the measurements. P-value was determined using excel and reported.

3.3 Results & Discussion

3.3.1 Lab-scale MEC fed with Acetate Synthetic Wastewater

3.3.1.1 Current Generation & COD Removal

Figure 3.3 presents cell voltage and $E_{cathode}$ against current density in the acetate-MEC at a HRT of 2, 4, 6, 8, 10, and 24 hrs. The current density tended to increase as HRT was decreased. The highest current densities were 8 ± 0.34 A/m^2 (p-value < 0.0001) and 8 ± 0.62 A/m^2 (p-value < 0.0001) at the HRT of 2 and 4 hrs, respectively. Lee, et al (2009) and Sleutel, et al (2011) reported that the current density is the function of substrate-utilization rate. Because decreasing the HRT in the completely-mixing MECs lead to high substrate concentration, a shorter HRT improves current density in MECs (An & Lee, 2013). The cell voltages ranged from 0.75 ± 0.16 (p-value < 0.0001) to 1.3 ± 0.16 V (p-value < 0.0001) . These results indicate low energy requirement for

the operation of the lab-scale MEC. In addition, the $E_{cathode}$ in the acetate-fed MEC ranged from -1.08 ± 0.86 V (p-value < 0.0001) to -1.69 ± 0.15 V (p-value < 0.0001) within the range of the HRTs. Considering that the standard potential at pH 7 for the O_2 reduction to H_2O_2 is +0.26 V (equivalent to -0.20 V vs Ag/AgCl) as shown in reaction (3.2), the $E_{cathode}$ in the acetate-MEC implies cathode overpotentials, which ranged from 0.72 to 1.49 V.

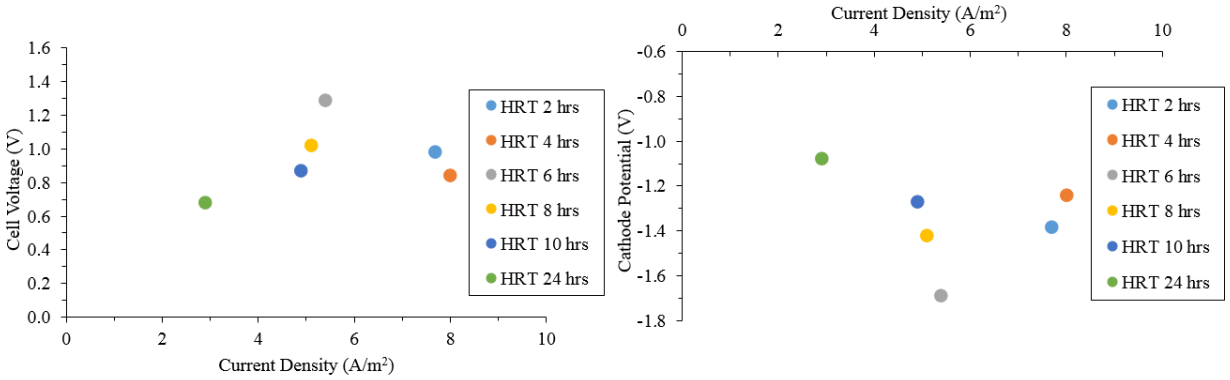

Figure 3.3: Cell voltage (left) and the cathode potential (right) against current density in the acetate-fed MEC at different HRTs.

Table 3.1 includes the COD removal efficiency (Rt) and coulombic efficiency in the acetate-fed MEC at different HRTs. The Rt improved as the HRT was prolonged. At a prolonged HRT, the ARB is capable of oxidizing more substrates, improving the R_t. The result indirectly reveals the importance of the HRT in the anode chamber of MECs to achieve the desirable effluent quality.

The coulombic efficiency in the acetate-MEC ranged from 37 to 82 %. These results indicated that a considerable amount of the substrate were consumed by non-ARB (i.e. methanogens) (Parameswaran, et al., 2009; Chae, et al., 2010). In other words, the electrons available in the substrate for the ARB to generate the current in MECs were rather lost to the electron sinks, such

as methane. Parameswaran, et al (2009) and Chae, et al (2010) pointed out the significance of suppressing the methanogens to improve the coulombic efficiency and showed the improved coulombic efficiency when the methanogenesis was intently inhibited with 2-bromoethane sulfonic acid (BES).

Table 3.1: COD concentration in the influent and the effluent, COD removal efficiency (R_t) and coulombic efficiency at different HRTs.

HRT (hr)	COD_{inf} (mg/L)	COD_{eff} (mg/L)	R_t (%)	Coulombic efficiency (%)
24	308 ± 4	20 ± 5	94 ± 2	82 ± 2
10	314 ± 3	52 ± 3	84 ± 1	64 ± 1
8	325 ± 1	70 ± 2	78 ± 5	55 ± 4
6	311 ± 1	85 ± 9	73 ± 3	49 ± 2
4	317 ± 8	105 ± 1	67 ± 3	52 ± 3
2	309 ± 4	168 ± 2	45 ± 2	37 ± 2

*Note: p-value for the parameters were smaller than 0.0001.

3.3.1.2 H_2O_2 Concentration & H_2O_2 Conversion Efficiency

Figure 3.4 shows the cumulative H_2O_2 concentration and the H_2O_2 conversion efficiency at 6 hr and 24 hr of the cathode operation for each HRT (*refer to Figure A.1 in the appendix for plots of the H_2O_2 evolution at each HRT*).

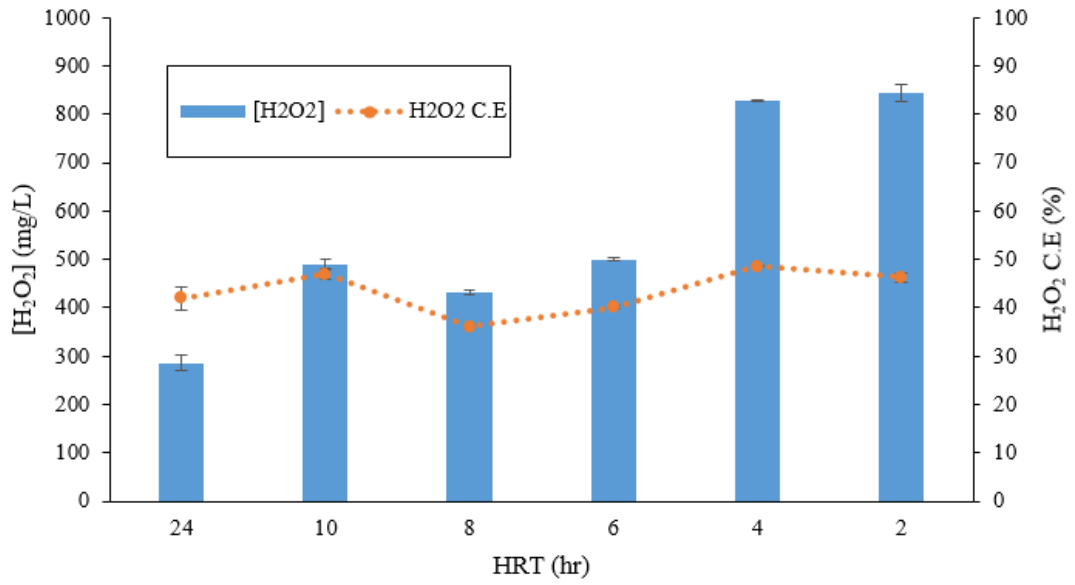

Figure 3.4: Cumulative H_2O_2 concentration and H_2O_2 conversion efficiency at 6 hr of cathode operation in the acetate-fed MEC at different HRTs (bars represent standard deviation).

At 6 hr of cathode operation, higher cumulative H_2O_2 concentration was found at a shorter HRT. The maximum cumulative H_2O_2 concentration at 6 hr of cathode operation was 843.50 ± 17.30 ($p < 0.0001$) and 830.44 ± 1.66 mg/L ($p < 0.0001$) at the HRT of 2 and 4 hrs, respectively; while the minimum cumulative H_2O_2 concentration of 285.56 ± 16.17 mg/L ($p = 0.0011$) was found at the HRT of 24 hrs. The increased H_2O_2 production rate at a shorter HRT pertains to the fact that the current density was higher at a shorter HRT (Figure 3.3). These results support that HRT is an operating parameter of interest to achieve a targeted H_2O_2 concentration in H_2O_2-producing MECs. Unlike the cumulative H_2O_2 concentration, the H_2O_2 conversion efficiency were comparable within the range of the HRT; the H_2O_2 conversion efficiency ranged from 36.15 ± 0.39 ($p < 0.0001$) to 46.31 ± 0.95 % ($p < 0.0001$). These results indicated that the considerable amount of the electrons produced from acetate oxidation was converted to H_2O_2.

Figure 3.5 presents the cumulative H_2O_2 concentration and H_2O_2 conversion efficiency at 24 hr of cathode operation for each HRT. At 24 hr of cathode operation, the highest cumulative H_2O_2 concentrations of 1447.14 ± 17.90 mg/L ($p < 0.0001$) was observed at the HRT of 6 hrs, which was followed by 10 hrs (1427.48 ± 24.42 mg/L, $p < 0.0001$), 8 hrs (1338.11 ± 18.57 mg/L, $p < 0.0001$), 4 hrs (1300.29 ± 10.98 mg/L, $p < 0.0001$), 2 hrs (1293.82 ± 23.39 mg/L, $p = 0.0001$), and 24 hrs (967.47 ± 1.87 mg/L, $p < 0.0001$).

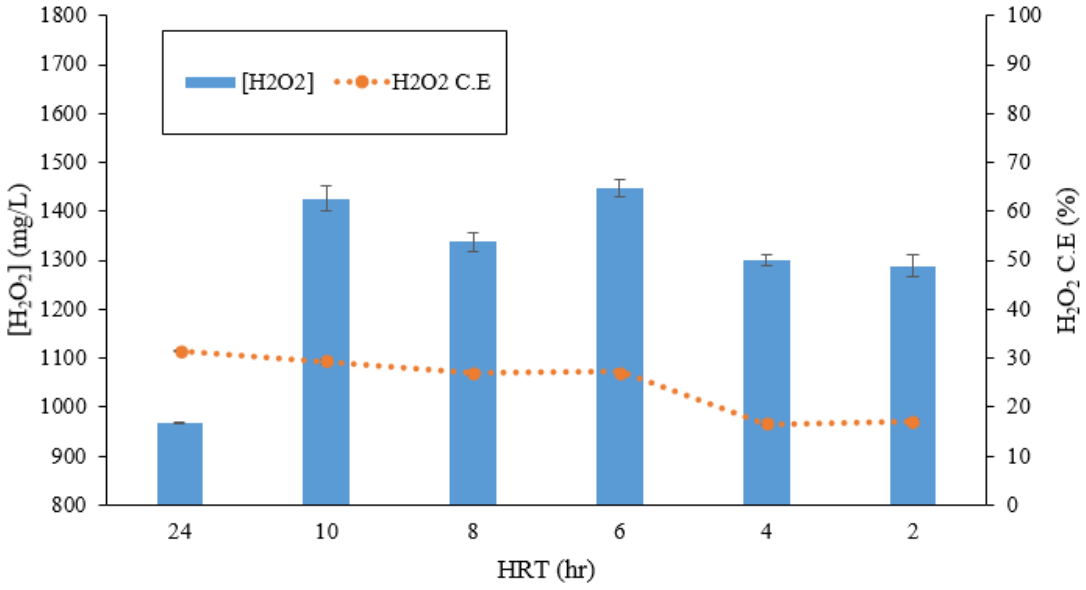

Figure 3.5: Cumulative H_2O_2 concentration and H_2O_2 conversion efficiency after 24 hrs of cathode operation in the acetate-fed MEC at different HRTs (bars represent standard deviation).

Interestingly, the H_2O_2 conversion efficiencies at 24 hr of cathode operation were lower than those at 6 hr of the cathode operation for all HRTs as shown in Figure 3.5; the H_2O_2 conversion efficiency ranged from 15.83 ± 0.29 % ($p = 0.0001$) to 31.48 ± 0.06 % ($p < 0.0001$). The decline in the H_2O_2 conversion efficiency can be attributed to the increased occurrence of H_2O_2 destruction

via the self-decomposition of H_2O_2 and reduction of H_2O_2 to H_2O. Qiang, et al (2002) studied the relation between self-decomposition of H_2O_2 and pH, and reported that self-decomposition of H_2O_2 was significant at high pH (pH > 9). As illustrated in Table 3.2, the pH in the cathode immediately became alkaline (pH > 11) within first 30 min of operation for each experiment due to the H^+ consuming reactions (O_2 reduction to H_2O_2, O_2 reduction to H_2O, and H_2 formation).

Table 3.2: Change in the catholyte pH over 24 hr-operation of the acetate-fed MEC at different HRTs.

Time	HRT (hrs)					
(min)	24	10	8	6	4	2
0	6.60	6.70	6.58	6.58	6.59	6.70
30	11.33	11.02	11.36	11.04	11.21	11.08
60	11.46	11.11	11.74	11.32	10.82	11.28
90	11.49	11.40	11.96	11.46	11.75	11.86
120	11.49	11.62	12.10	11.71	12.04	11.98
150	11.52	11.64	12.18	11.92	11.87	11.98
180	11.53	11.98	12.26	12.12	11.90	12.02
210	11.53	11.95	12.30	12.16	12.06	12.03
240	11.51	11.96	12.40	12.38	11.96	12.09
360	11.43	12.02	12.55	12.64	12.05	12.25
540	11.48	12.43	12.72	12.84	12.15	12.52
1440	11.59	12.86	12.95	13.00	12.50	12.89

The occurrence of H_2O_2 self-decomposition was likely to occur at the high pH. Despite the self-decomposition of H_2O_2 at high pH, the linear H_2O_2 generation in 6 hrs of cathode operation was observed (Figure A.1). This indirectly indicates that H_2O_2 production rate was faster than H_2O_2 self-decomposition rate until 6 hrs of cathode operation. However, as H_2O_2 was accumulated in the cathode with time, the reaction of H_2O_2 reduction to H_2O was triggered and, eventually, the rate of H_2O_2 destruction via both H_2O_2 reduction to H_2O and H_2O_2 self-decomposition outpaced

the rate of H_2O_2 production. For this reason, it is probable that H_2O_2 conversion efficiency decreased with time although the current density remained steady for each operation.

3.3.2 Lab-scale MEC fed with Domestic Wastewater

3.3.2.1 Current generation & COD removal

Figure 3.6 shows the average cell voltage and the cathode potential against current density in the wastewater-MEC (initial COD: 510.21 ± 15.18 mg/L) at the HRT of 2, 6, and 10 hrs.

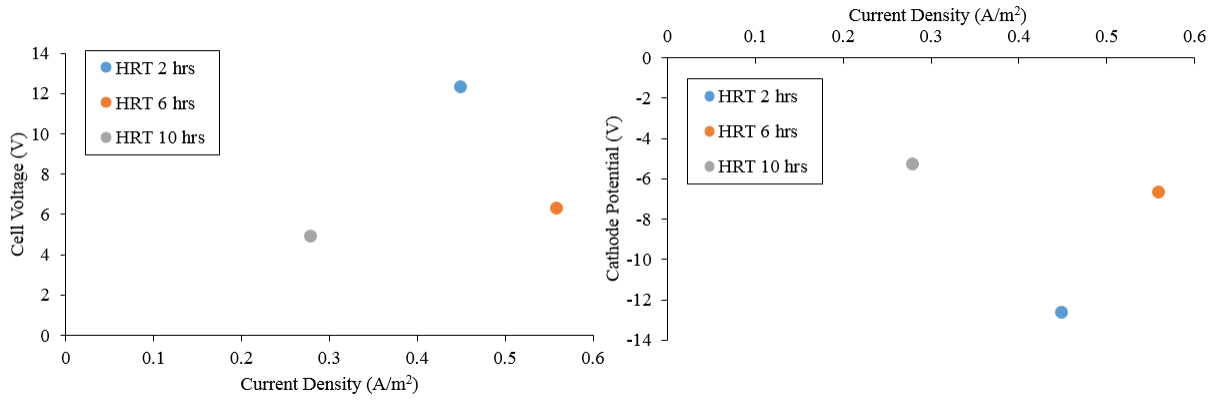

Figure 3.6: Cell voltage (left) and cathode potential (right) against current density in the wastewater-MEC at a different HRT.

There was a discrepancy in the current density at each HRT. However, the effect of the HRT on the current density was insignificant. In comparison to the current densities in the acetate-fed MEC, the current densities in the wastewater-fed MEC were substantially low ranging from 0.3 ± 0.05 ($p < 0.0001$) to 0.56 ± 0.15 A/m^2 ($p < 0.0001$). Modin & Fukushi, (2012) suggested that ARB may be limited to the oxidation of acetate and lack the ability of oxidizing other substrates because the ARB were acclimated to acetate. In addition, Dhar, et al (2014) reported biodegradability and particulate matter in wastewater as the crucial features that lower the current density in wastewater-

fed MECs. As illustrated in Figure 3.6, the cell voltages in the wastewater-fed MEC at different HRTs were high, indicating substantial energy losses in the wastewater-fed MEC. It is expected that ohmic resistance in the wastewater-fed MEC would be severe due to membrane fouling. It is likely that the membrane fouling is due to the presence of the particulate matter in real wastewater. At a shorter HRT, hydrolysis and fermentation of complex organic compounds into simple forms (i.e. acetate) would be limited, accentuating the membrane fouling at a short HRT. This supports the substantial high cell voltage (or energy losses) at a short HRT.

As Table 3.3 shows, the MEC attained the efficient COD removal when the wastewater was fed. It is apparent that COD removal improved with the increasing HRT. Also, the coulombic efficiency was considerably low at the HRT of 10, 6, and 2 hrs, respectively. In other words, non-ARB (i.e. fermentation and methanogenesis) contributed to the majority of the COD removed in the raw wastewater fed into the MEC.

Table 3.3: COD concentration in the influent and the effluent, COD removal efficiency and coulombic efficiency in the wastewater-fed MEC at different HRTs

HRT (hr)	COD_{inf} (mg/L)	COD_{eff} (mg/L)	R_t (%)	Coulombic efficiency (%)
10	509 ± 80	182 ± 24	64 ± 50 (p = 0.016)	3 ± 0.2 (p = 0.004)
6	509 ± 80	203 ± 14	60 ± 30 (p = 0.014)	4 ± 0.2 (p = 0.020)
2	511 ± 23	313 ± 34	39 ± 70 (p = 0.008)	2 ± 0.3 (p = 0.041)

3.3.2.2 H_2O_2 Concentration & H_2O_2 Conversion Efficiency

Figure 3.7 presents the cumulative H_2O_2 concentration and the H_2O_2 conversion efficiency at 6 hr and 24 hr of cathode operation in the wastewater-fed MEC at the HRT of 10, 6, and 2 hrs.

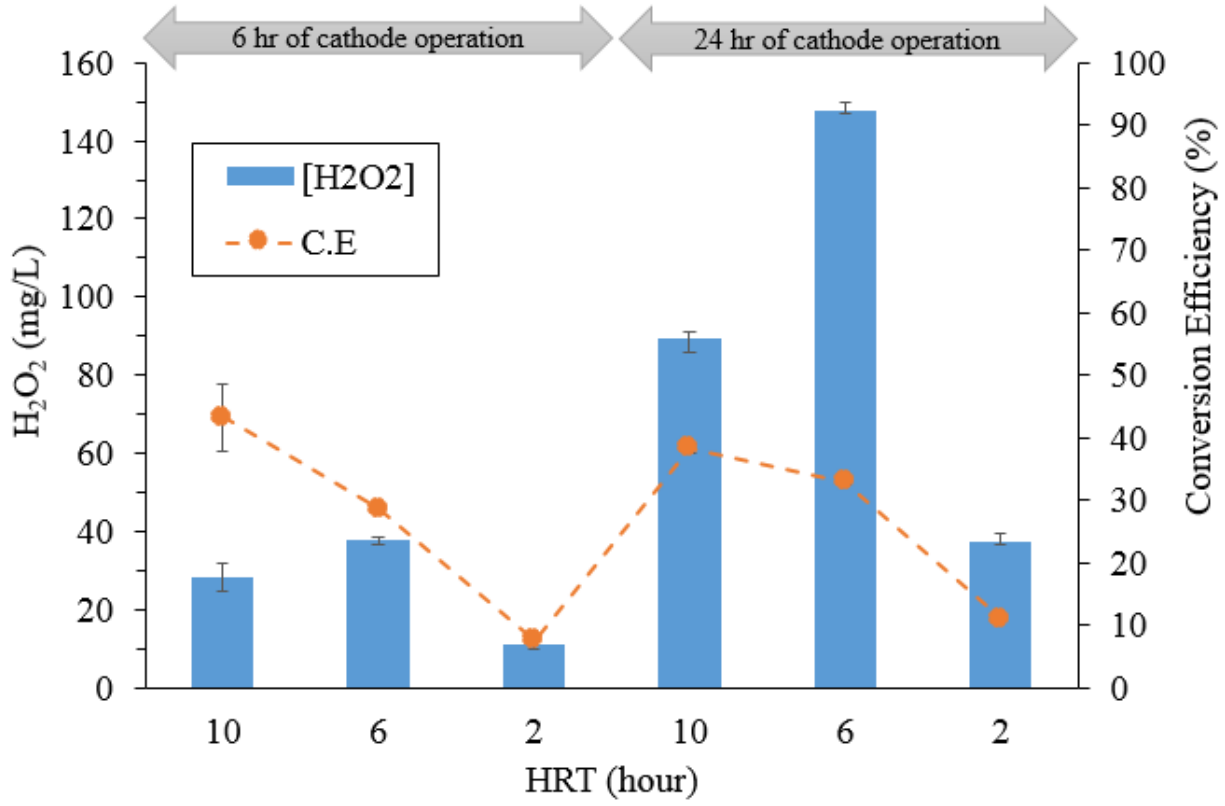

Figure 3.7: Cumulative H_2O_2 concentration and H_2O_2 conversion efficiency at 6 hr and 24 hr of cathode operation for the wastewater-fed MEC at the HRT of 10, 6, and 2 hrs.

Over 24-hr operation for each experiment, H_2O_2 production was substantially low at all HRTs. The low H_2O_2 production in the wastewater-MEC is mainly due to low current densities (Figure 3.6). This highlighted the importance of the further research that are focused on improving current density in MECs fed with real wastewater.

The H_2O_2 conversion efficiency were relatively consistent throughout each operation. Similar to the acetate-fed MEC, the wastewater-fed MEC also exhibited the immediate rise in the catholyte pH (Table 3.4). This poses the potential occurrence of H_2O_2 self-decomposition at high pH. Nonetheless, the H_2O_2 conversion efficiency at 6 hr of the cathode operation was 43 % ($p = 0.005$)

at the HRT of 10 hrs and 28 % ($p = 0.0002$) at the HRT of 6 hrs while the H_2O_2 conversion efficiency at 24 hr of the cathode operation were 38 % ($p = 0.002$) and 32 % ($p = 0.003$) at the HRT of 10 and 6 hrs, respectively. The small change in the H_2O_2 conversion efficiency over time under the operating conditions indicated insignificant occurrence of side reactions. It is interesting to observe that the H_2O_2 conversion efficiency at the HRT of 2 hrs were low; it was close to 10 % throughout the operation. The low H_2O_2 conversion efficiency at the HRT of 2 hrs can be attributed to the high $E_{cathode}$, which may have triggered the side reactions (i.e. O_2 reduction to H_2O, and H_2O_2 reduction to H_2O, and H_2 reaction).

Table 3.4: Change in the catholyte pH over 24 hr of operation of the wastewater-fed MEC at different HRTs.

Time	HRT		
(min)	2	6	10
0	6.6	6.58	6.59
360	11.11	11.23	10.74
1440	11.37	11.38	10.84

3.4 Conclusions

In this study, the lab-scale MEC was operated to demonstrate H_2O_2 production under different operating conditions, such as feeds and HRTs. The evaluation of the lab-scale MEC for wastewater treatment and H_2O_2 production was carried out when the system was fed with 1) acetate synthetic wastewater at the HRT ranging from 2 to 24 hrs and 2) domestic wastewater at the HRT ranging from 2 to 10 hrs.

The performance of the acetate-fed MEC was influenced by HRT. The COD removal efficiency increased as the HRT increased; the acetate-fed MEC achieved the highest COD removal

efficiency of 94 ± 2 % at the HRT of 24 hrs and the lowest COD removal efficiency of 45 ± 2 % at the HRT of 2 hrs. The coulombic efficiency ranged from 37 ± 2 to 82 ± 2 % for the range of the HRTs, indicating that ARB were responsible for the majority of the COD removed in the acetate synthetic wastewater. This resulted in the current density ranging from 2.9 ± 0.3 (at the HRT of 24 hrs) to 8.0 ± 0.6 A/m^2 (at the HRT of 2 hrs). Also, the acetate-MEC showed high H_2O_2 production; the highest cumulative H_2O_2 concentration at 6 hrs of cathode operation was 843.50 ± 17.30 mg/L at the HRT of 2 hrs. However, the accumulation of H_2O_2 and high pH (pH >8) in the cathode over time triggered self-decomposition of H_2O_2 and H_2O_2 reduction to H_2O.

Similar to the acetate-fed MEC, the wastewater-fed MEC also experienced the increasing COD removal efficiency as the HRT increased. The highest COD removal efficiency of 64 ± 5 % was observed at the HRT of 10 hrs, and the lowest COD removal efficiency of 39 ± 9 % was observed at the HRT of 2 hrs. However, non-ARB (i.e. fermenters and methanogens) was held accountable for the majority of the COD removed in the wastewater-fed MEC. This resulted in low current densities; the current density in the wastewater-fed MEC ranged from 0.30 ± 0.05 to 0.60 ± 0.05 A/m^2, which were lower than the current densities in the acetate-fed MEC. This led to low H_2O_2 production. The highest cumulative H_2O_2 concentration in the wastewater-fed MEC was 147.73 ± 1.98 mg/L at 24 hrs of cathode operation at the HRT of 6 hrs. The operation of the lab-scale MEC proved its promising potential for high H_2O_2 production; however, low current density and H_2O_2 production in the wastewater-fed MEC indicated the importance of future study to focus on improving current generation and H_2O_2 production when real wastewater is used as the feed for MECs.

4. H_2O_2 production in a pilot-scale Microbial Electrochemical Cell

Abstract

Despite the growing attention of MEC application for on-site H_2O_2 production, no up-to dated MEC pilot studies focused on H_2O_2 production. In this study, the pilot-scale MEC was operated in batch mode and evaluated for H_2O_2 production when fed with acetate synthetic wastewater. This study consisted of two phases: the pilot MEC was equipped with an anion exchange membrane (AEM-MEC) in phase I and with a cation exchange membrane (CEM-MEC) in phase II to mitigate proton accumulation in an anode chamber of the MEC.

The AEM-MEC and CEM-MEC required a small applied voltage from 0.35 to 1.9 V for the operation. The current densities in the pilot system were commonly low with the maximum current density of 0.94 and 0.96 A/m^2 for the AEM-MEC and CEM-MEC, respectively. The CEM-MEC exhibited slightly better H_2O_2 production probably due to the continuous proton (H^+) transfer from the anode the cathode through the membrane; the cumulative H_2O_2 concentration was 9.0 ± 0.38 mg/L and 98.48 ± 1.6 mg/L in the 20-day operation of the AEM-MEC and the 15-day operation of the CEM-MEC, respectively. Nonetheless, the two MECs showed extremely low H_2O_2 conversion efficiency, which ranged from 0.20 ± 0.03 to 0.35 ± 0.05 % and from 4.1 ± 0.07 to 7.2 ± 0.09 % in the AEM-MEC and CEM-MEC, respectively. These results indicate significant H_2O_2 loss via H_2O_2 self-decomposition or H_2O_2 reduction to H_2O. While the operation of the pilot system demonstrated H_2O_2 production in a pilot-scale MEC, it has presented the technical (low current generation and H_2O_2 conversion efficiency) and design (membrane expansion, the CGC, CO_2 trapping) challenges of the pilot system and conveyed the need for further studies that address these challenges.

4.1 Introduction

An MEC is considered as a potential sustainable platform for the energy-efficient wastewater treatment, as it enables the recovery of the value-added products (i.e. electricity, H_2 and H_2O_2), together with organic stabilization. Due to its potential as sustainable, energy-efficient wastewater treatment technology, MECs has garnered the growing attention by the research communities in the last decade (Zhang & Angelidaki, 2014). Although the up-to-dated studies on the technology would possibly provide a sound foundation to achieve the successful scale-up of MECs for the practical applications, the majority of them were conducted at a laboratory scale. To attain the successful implementation of the MEC towards the practical applications, the pilot studies on the technology are vital.

In spite of the fact that the majority of the up-do-dated studies used laboratory-scale MECs, several researchers had operated large-scale MECs (Cusick, et al., 2011; Gil-Carrera, et al., 2013[a]; Gil-Carrera, et al., 2013[b]; Zhang, et al., 2013). However, none of the studies has targeted H_2O_2 production from MECs at a large-scale. Rather, they focused on either electricity production or H_2 production, which failed to give significant benefit against substantial operating and maintenance costs. In comparison, H_2O_2 generated on-site using MECs can be reused for improving water quality or oxidizing specific compounds in waste and wastewater treatment. Hence, the MECs producing H_2O_2 have significant implications in clean technologies due to energy efficiency, cost benefit, and sustainability, which can accelerate the practical application in the near future.

In this study, a pilot-scale MEC was operated in batch mode and evaluated in two phases. The pilot-scale MEC was equipped with an anion exchange membrane (AEM) in phase I and with a

cation exchange membrane (CEM) in phase II. Chapter 4 includes the evaluation of the pilot system in terms of wastewater treatment efficiency and H_2O_2 production, and it also presents a discussion with regard to the performance of the pilot system. Technical and design challenges of the pilot MEC were identified, and possible solutions corresponding to each problem were suggested in this chapter.

4.1 Material & Method

4.1.1 Reactor Configuration

Figure 4.1 presents the schematic diagram and the picture of the pilot-scale MEC installed at the Waterloo Environmental Biotechnology (WEB) laboratory. The system has a dual-chamber configuration; it is comprised of an anode and the cathode chamber. The anode chamber had the dimension of 1 m x 0.5 m x 0.2 m and the cathode chamber had the dimension of 1 m x 0.5 m x 0.2 m, projecting the designed volume of 100 L and 10 L, respectively.

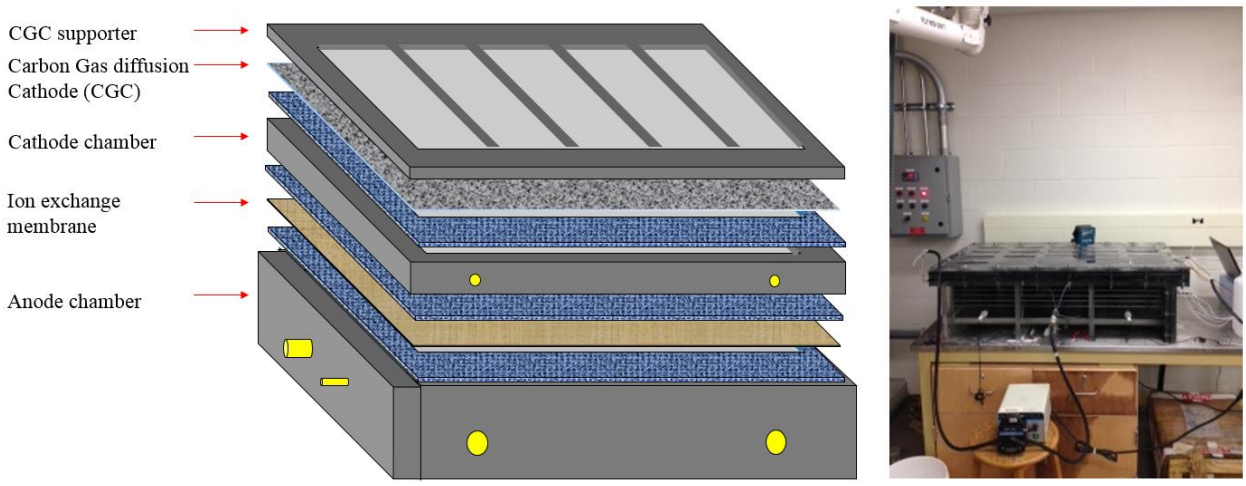

Figure 4.1: Schematic diagram (left) and the picture (right) of the pilot-scale MEC.

Although the pilot system was designed to have the working volume of 100 L and 10 L for the anode and the cathode compartment, respectively, there was an unexpected issue of the membrane expansion due to the weight of the catholyte (Figure 4.2). This resulted in the reduction of the working volume for the anode compartment (from 100 L to 85 L) and expansion of the working volume for the cathode compartment (from 10 L to 25 L). The issue of membrane expansion would potentially lead to other unexpected problems (more discussion in Results and Discussion). Membrane supporters would be required to prevent the membrane expansion in pilot-scale MECs with a similar configuration (Figure 4.3). This issue must be taken into consideration for the novel design of the pilot-scale MEC for H_2O_2 production.

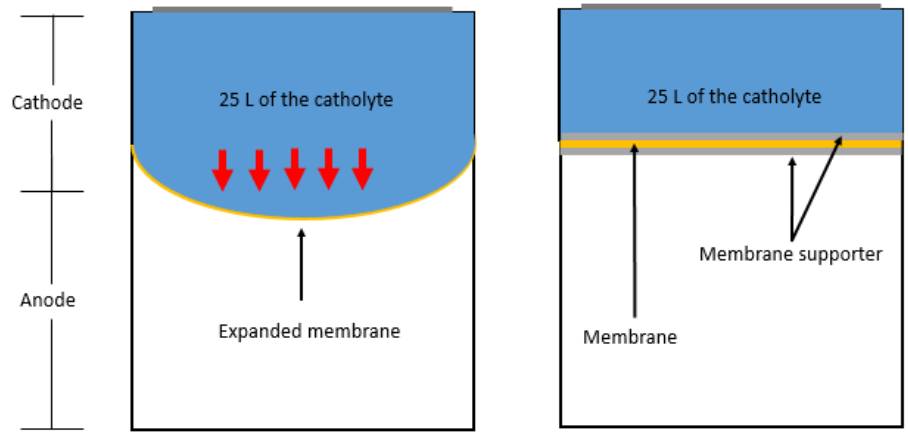

Figure 4.2: Membrane expansion in the pilot-scale MEC (left) and proposed membrane supports (right).

With the primary focus on improving the current generation within the pilot-scale system, the anode chamber was designed as shown in Figure 4.3. In order to increase the surface area for the ARB biofilm formation, five anode modules were incorporated into the anode chamber (Figure 4.3). Each anode module was high density carbon fibers (2293-A, 24A Carbon Fiber, Fibre Glast

Development Corp., Ohio, USA) connected with a stainless steel frame. The carbon fibers were pretreated to improve the ARB attachment by immersing in nitric acid (1 N), acetone (1 N), and ethanol (1 N) each for 1 day in sequence, and washed thoroughly with de-ionized water. To incur the mixing conditions in the anode, a pump was used to circulate the anolyte at the flow rate of 2 L/min.

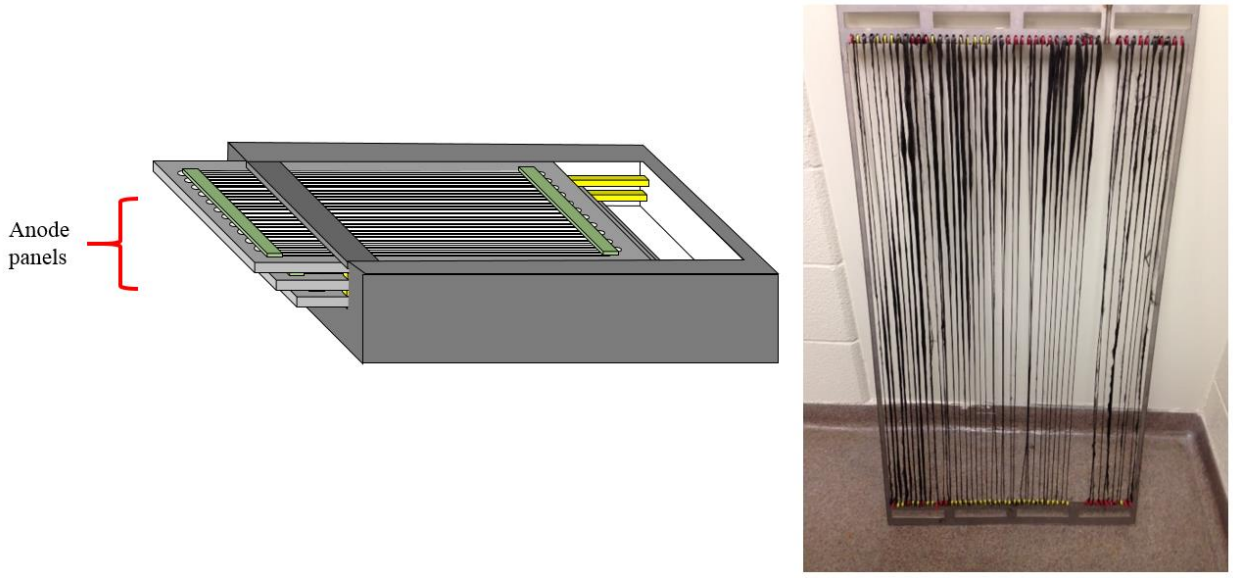

Figure 4.3: Schematic diagram of the anode chamber (left) and the picture of the anode panel (right).

For the cathode, the CGC (GD2230, Fuel Cell Earth, USA) was used. The passive aeration was implemented for the CGC, creating the 2-cm spacing between the membrane and the cathode. A cation exchange membrane (CEM) (CMI-7000, Membranes International Inc., USA) and an anion exchange membrane (AEM) (AMI-7001, Membranes International Inc., USA) with the surface area of 0.5 cm^2 were compared for the MEC. The use of the CEM allows protons (H^+) to travel from the anode to the cathode for charge neutrality. In comparison, the use of the AEM allows

hydroxyl ions (OH^-) in the cathode chamber to move to the anode for charge neutrality. The setback of utilizing a CEM for the MEC is the gradual pH drop in the anode because other cations (e.g., Ca^{2+}, Mg^{2+}, Na^+, etc), instead of protons, transfer to the cathode. The movement of other cations results in proton accumulation in the anode, and eventually inhibits ARB metabolism (Torres, et al., 2008). On the other hand, AEM is able to keep neutral pH in the anode since OH^- transport from the cathode to the anode; OH^- react with protons accumulated from organic oxidation by ARB in the anode, and this maintains neutral pH in the anode. Therefore, the AEM could minimize the inhibition of the ARB activity due to pH drop (Kim, et al., 2007).

For the online-monitoring of the cell voltage and the electrode potentials, a saturated calomel electrode (SCE) (MF-2052, Bioanalytical System Inc. (BASI), USA) was used in the anode chamber and, thus, the electrode potentials are reported relative to SCE reference electrode in this chapter. The anode modules and the cathode were connected to a data logging system (Keithly 2700, Keithley Instruments, Inc. USA)). The power supply (Array 3654A, Array Electronic co., LTD, China) was utilized as an external energy input. Also, a pH probe was placed in the anode to monitor the pH.

4.1.2 Operation

To optimize the current generation in the pilot-scale MEC, it is imperative to form ARB biofilm that is highly active in consuming substrates; thus, ARB acclimation is an important step for the operation of a pilot-scale MEC. To acclimate ARB, the acetate medium was prepared. The composition of the medium was (per L of tap water) 2050 mg/L CH_3COONa, 2274 mg KH_2PO_4, 11,678 mg $Na_2HPO_4 \cdot 12H_2O$, 37 mg NH_4Cl, 25 mg $MgCl_2 \cdot 6H_2O$, 6 mg $MnCl_2 \cdot 4H_2O$, 0.1 mg

$CuSO_4 \cdot 5H_2O$, 0.1 mg $Na_2WO_4 \cdot 2H_2O$, 0.1 mg $NaHSeO_3$, 0.01 mg $CaCl_2 \cdot 2H_2O$, 0.5 mg $ZnCl_2$, 0.1 mg $AlK(SO_4)_2$, 0.1 mg H_3BO_3, 0.1 mg $Na_2MoO_4 \cdot 2H_2O$, 0.2 mg $NiCl_2$, 5 mg EDTA, 1 mg $CO(NO_3)_2.6H_2O$, and 0.2 mg $NiCl_2 \cdot 6H_2O$. The medium was sparged with ultra-pure nitrogen (99.999%) for 30 min. Then, $FeCl_2 \cdot 2H_2O$ (20 mM) and $Na_2S \cdot 9H_2O$ (77 mM) were added to the medium (1 mL per L). Medium pH was constant at 7.3 ± 0.1. The effluent from the existing lab-scale MECs were inoculated for the ARB growth. Due to the limitation on the amount of the effluent that could be obtained from the lab-scale MECs daily, 500 mL of the effluent was inoculated daily for 7 days, totaling 3.5 L of the effluent inoculated into the anode. The cathode chamber was filled with tap water.

When the steady current density of 0.9 A/m^2 was reached, the experiments were initiated. The operation of the pilot-scale MEC was divided into two phases in which 20 mM acetate synthetic wastewater was used as the feed for the maximum current generation from the pilot system. In phase I, the pilot system equipped with the AEM (AEM-MEC) was operated in batch mode. In the following phase (phase II), the pilot system with the CEM (CEM-MEC) was operated in batch mode.

4.1.3 Analytical method and Computation

For the measurement of H_2O_2 concentration and the calculation of H_2O_2 conversion efficiency, refer to chapter 2.2.3. Also, the identical analytical method for the COD measurement was used, which is described in chapter 3.2.4.

Statistical analysis was performed based on H_2O_2 and COD measurements in triplicate. Refer to Chapter 3.4.1 for statistical analysis.

4.2 Results & Discussion

4.2.1 Cell Voltage, Anode & Cathode Potential, and Current Density

Figure 4.4 and Figure 4.5 shows the cell voltage and $E_{electrode}$ (both anode and the cathode) for the pilot-scale MEC when equipped with the AEM and the CEM, respectively.

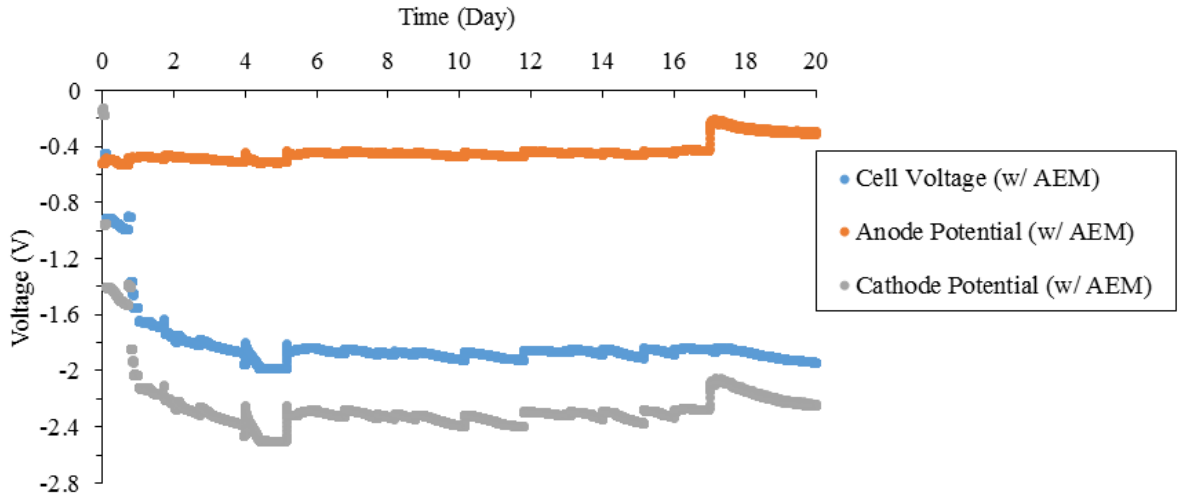

Figure 4.4: Cell voltage and electrode potential in the AEM-MEC.

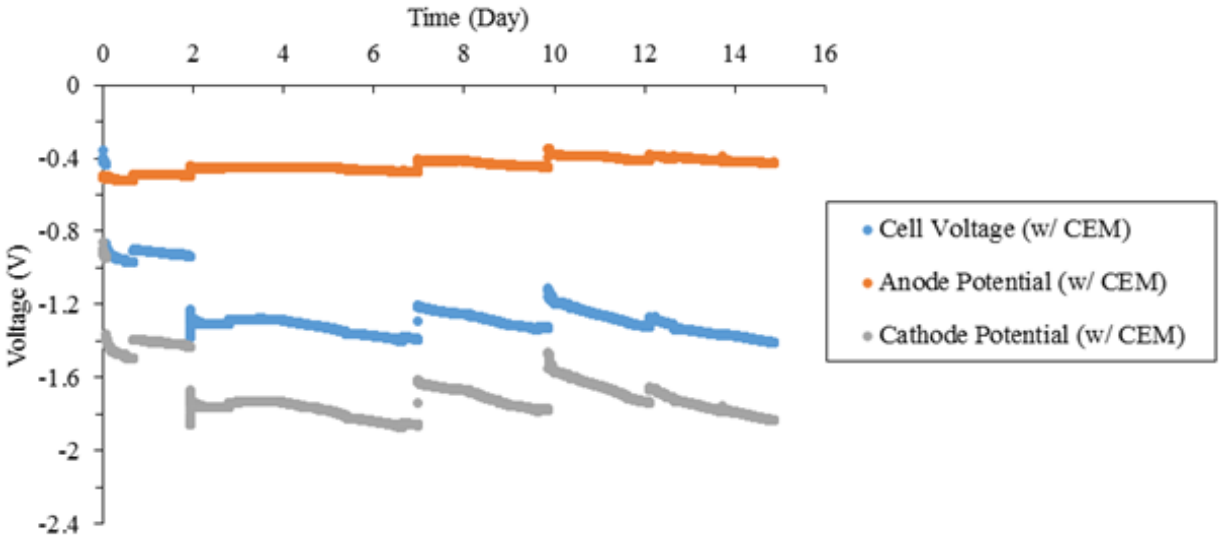

Figure 4.5: Cell voltage and electrode potential in the CEM-MEC.

The E_{anode} in the AEM-MEC and the CEM-MEC was controlled between -0.3 and -0.5 V (vs SCE) to establish the optimal E_{anode} for the growth of the ARB (Aelterman, et al., 2008; Lee, et al., 2009; Torres, et al., 2009). The corresponding $E_{cathode}$ ranged from -2.0 to -2.4 V and from -1.4 to -2.0 V in the AEM-MEC and the CEM-MEC, respectively. The $E_{cathode}$ in both operations of the pilot system were comparable to those (from -1.08 to -1.69 V) observed in laboratory-scale acetate-MEC (Figure 3.3). In both operations of the pilot-scale MEC, there were abrupt declines in the $E_{cathode}$ (on Day 1, 2, 3, 4, 5, 10, 12, 13, 14, 15, and 17 for the AEM-MEC, and Day 1, 2, 7, 10 and 12 for the CEM-MEC). Over the course of the operation, the CGC and the catholyte did not remain in complete contact due to the evaporation of the catholyte with time (Figure 4.6). Fresh catholyte had to be manually added to the cathode chamber to maintain the contact between the cathode and the catholyt. The pilot MEC was designed to install the CGC on the top of the system (Figure 4.2) because the paper-type CGC is extremely brittle with the thickness of 225 um and would not be able to support a large volume of the catholyte. However, positioning the cathode on the top presented the problem, which required the frequent maintenance of adding the catholyte.

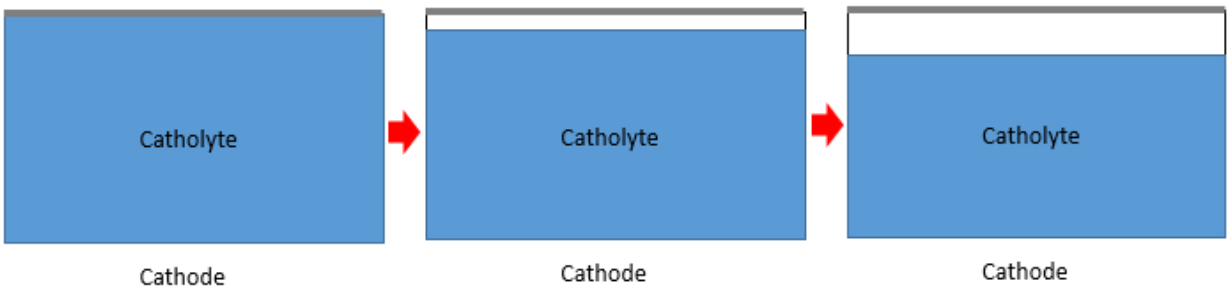

Figure 4.6: Water evaporation over time in the cathode compartment.

The AEM-MEC and the CEM-MEC showed a slight difference in the cell voltage. The slightly lower cell voltage was observed in the CEM-MEC than in the AEM-MEC. The voltage ranging

from -0.45 to -1.99 V and from -0.35 to -1.4 V was applied to the AEM-MEC and the CEM-MEC, respectively.

Figure 4.7 and Figure 4.8 shows the current density evolution in 20-day operation of the AEM-MEC and 16-day operation of the CEM-MEC, respectively.

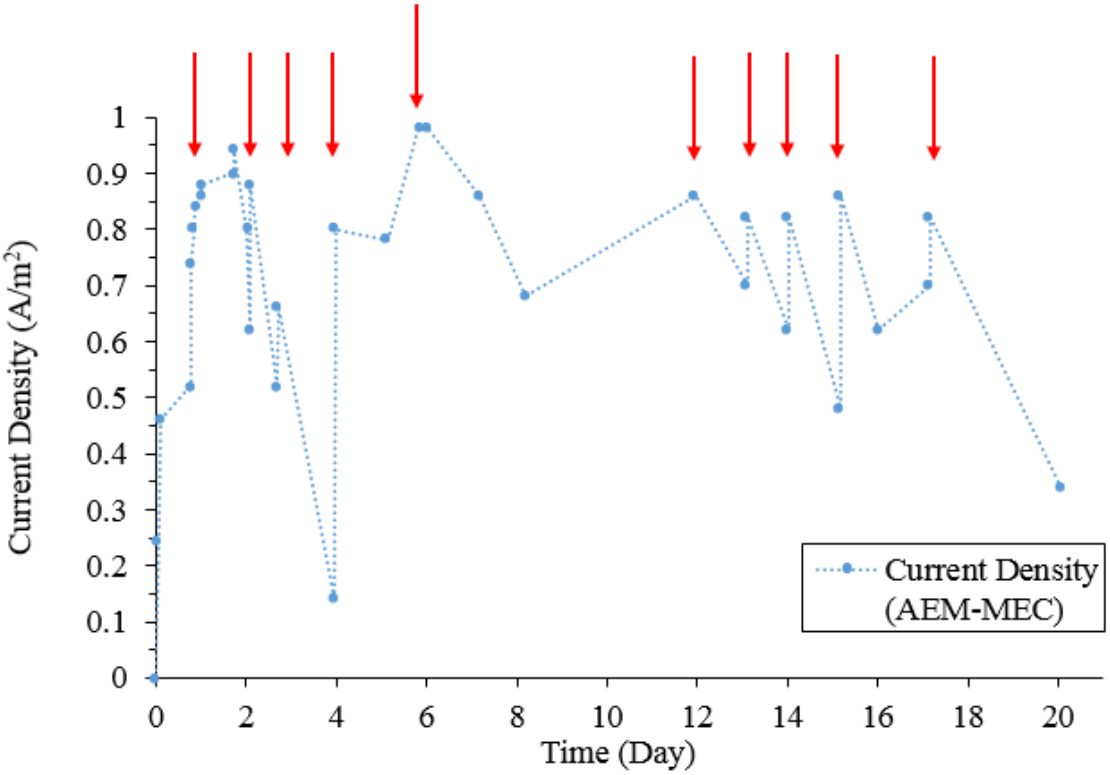

Figure 4.7: Current density in the 20-day operation of AEM-MEC. Red arrows indicate catholyte replacement.

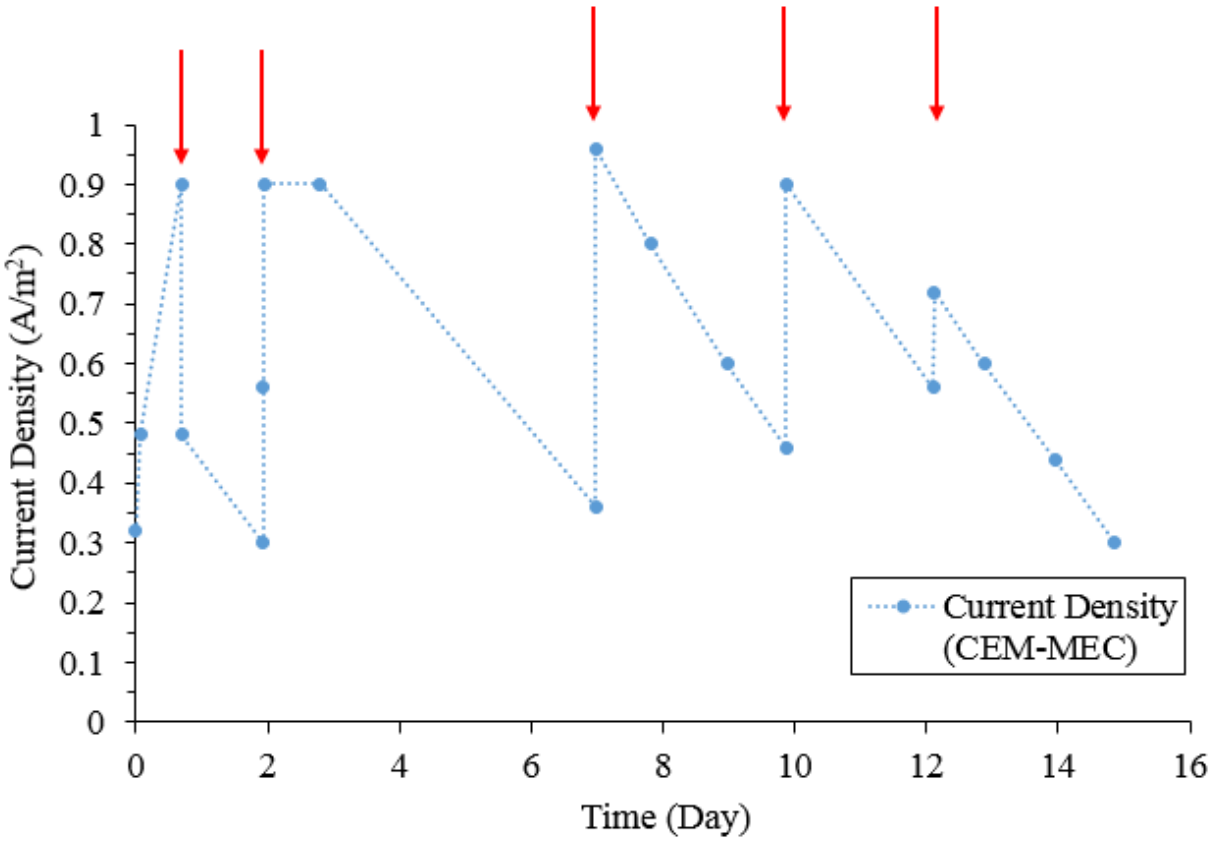

Figure 4.8: Current density in the 16-day operation of the CEM-MEC. Red arrows indicate catholyte replacement.

The maximum current density in the AEM-MEC and the CEM-MEC were comparable with 0.94 A/m^2 and 0.96 A/m^2, respectively. In both AEM-MEC and CEM-MEC, the fluctuations in the current density were observed. This was associated to the water evaporation that was discussed previously. The current density decreased as the catholyte gradually evaporated with time, and it increased steeply when the fresh catholyte was added to maintain the contact between the CGC and the catholyte (indicated with the arrows in Figure 4.7 and Figure 4.8). Therefore, the modifications to the design of the pilot-sale are necessary to allow for the long-term operation of the pilot-scale MEC with minimal maintenance and for the optimal performance.

4.2.2 COD Removal Efficiency

Figure 4.9 and Figure 4.10 shows the initial and the final COD concentration, which represent the acetate in the synthetic wastewater, in the AEM-MEC and the CEM-MEC, respectively. Because both experiments were carried out in batch operation (with the initial COD concentration of ~1000 mg/L), it was apparent that the effluent COD concentration gradually decreased with time in both AEM-MEC and CEM-MEC. The final COD concentration was 229 ± 1.0 mg/L with the COD removal efficiency of 77.17 ± 2.56 % ($p = 0.048$) at the end of the 20-day operation for the AEM-MEC and 503.76 ± 32.30 mg/L with the COD removal efficiency of 49.54 ± 3.13 % ($p = 0.01$) at the end of the 16 day-operation for the CEM-MEC. It is apparent that the substrate did not exhaust at the end of each operation and was adequate enough for ARB. However, the operations had to cease due to a pH drop, which will be discussed in the next chapter.

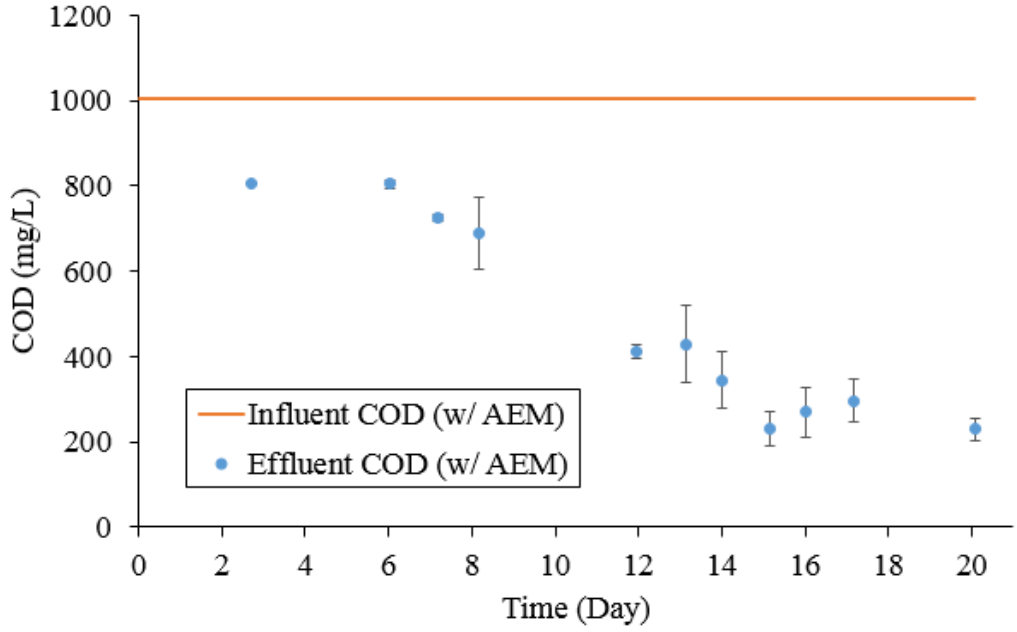

Figure 4.9: Influent and effluent COD concentration in the AEM-MEC (bars represent standard deviation).

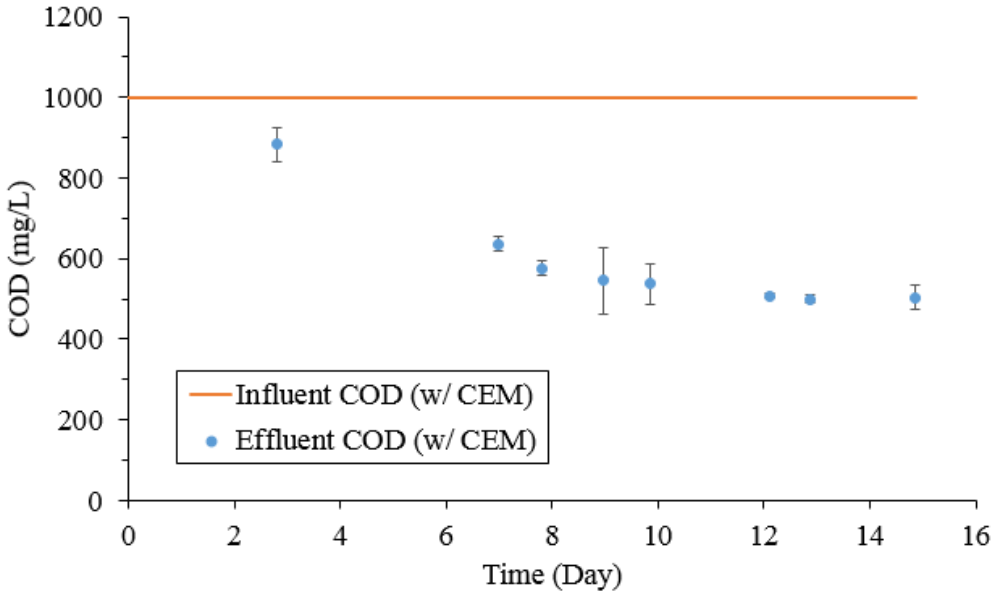

Figure 4.10: Influent and effluent COD concentration in the CEM-MEC (bars represent standard deviation).

4.2.3 pH & Conductivity

The pH of the anolyte and the catholyte was measured in the AEM-MEC and the CEM-MEC (Figure 4.11 and Figure 4.12).

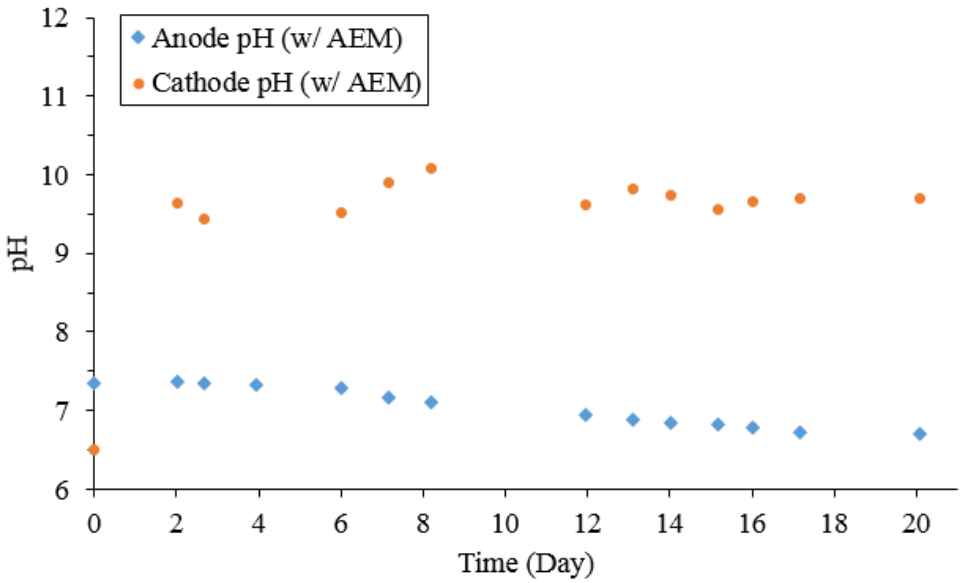

Figure 4.11: Anolyte and catholyte pH in the AEM-MEC.

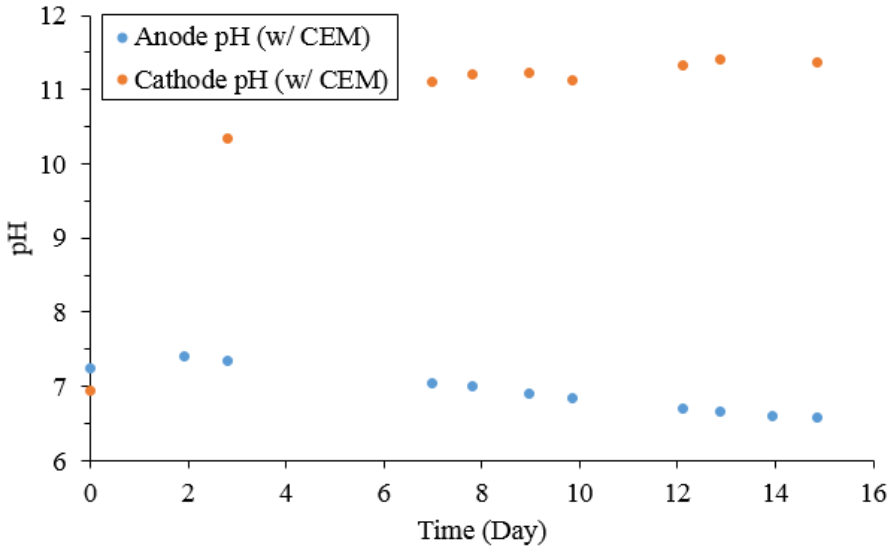

Figure 4.12: Anolyte and catholyte pH in the CEM-MEC.

In both AEM-MEC and CEM-MEC, it was observed that the anolyte pH was gradually decreasing with time. On Day 20, the anolyte pH in the AEM-MEC was decreased to 6.5; whereas, the anolyte pH in the CEM-MEC was 6.5 on Day 16. It has been reported that the anolyte pH below 6.5 would inhibit the ARB activity (Torre, et al., 2009). Therefore, the systems had to stop although the sufficient amount of the substrate (acetate) were still present on the system (Figure 4.9 and Figure 4.10).

Proton accumulation in the anode was not expected for the AEM-MEC because OH^- generated from O_2 reduction transfers from the cathode to the anode for charge neutrality. However, the anolyte pH in the AEM-MEC dropped from 7.3 to 6.5 in 20 days. This phenomenon in the AEM-MEC would result from CO_2 production through acetate oxdiation and accumulation in the anode. In the lab-scale MEC, the outlet was installed on the top of the MEC for the release of CO_2; however, in the pilot-scale MEC, no outlet was erroneously installed to release CO_2 (Figure 4.13). The absence of an outlet in the pilot-scale MEC resulted in the trap of CO_2, which was then dissolved in the anode and eventually reduced the anolyte pH in the AEM-MEC. For the same reason, the anolyte pH dropped in the CEM-MEC. However, the accumulation of H^+ in the anode chamber of the CEM-MEC occurred because other cations (i.e. Ca^{2+}, Mg^{2+} and Na^+), rather than H^+, transferred from the anode to the cathode in order to maintain the charge neutrality, and this also played a critical role in the declined anolyte pH. CO_2 and H^+ accumulation in the anode chamber of the CEM-MEC accelerated the drop in the anolyte pH, explaining a shorter term for the anolyte pH to drop below 6.5 in the CEM-MEC (16 days in the CEM-MEC vs 20 days in the AEM-MEC).

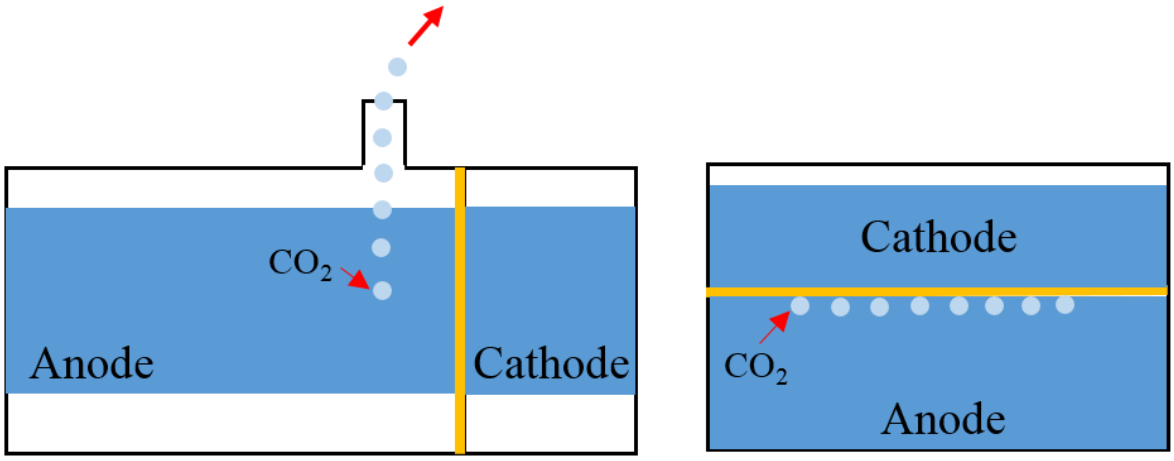

Figure 4.13: CO_2 released to the air in the lab-scale MEC and CO_2 trapped in the pilot-scale MEC.

The catholyte pH became alkaline immediately after the initiation of the experiment for both AEM-MEC and the CEM-MEC. The CEM-MEC experienced a gradual increase in the catholyte pH from 6.95 (on Day 1) to 11.36 (Day 15); whereas, the catholyte pH in the AEM-MEC was maintained at ~ 9.7 throughout the operation. The alkaline pH in the cathode chamber of both AEM-MEC and CEM-MEC would be due to the H^+ consuming reactions (i.e. O_2 to H_2O_2 and O_2 to H_2O) in the cathode. However, unlike the CEM-MEC in which the catholyte pH increased gradually with time, the AEM-MEC exhibited the catholyte pH that was maintained at ~9.7 throughout the operation. In the AEM-MEC, H^+ was consumed in O_2 reduction reaction to H_2O and H_2O_2, surging the catholyte pH; however, OH^- was transferred from the cathode to the anode for charge neutrality. This would eventually reach the equilibrium of chemical concentrations in the AEM-MEC and resulted in the consistent catholyte pH of the AEM-MEC at ~9.7.

Figure 4.14 and Figure 4.15 show the conductivity in the anode and the cathode of the AEM-MEC and CEM-MEC, respectively.

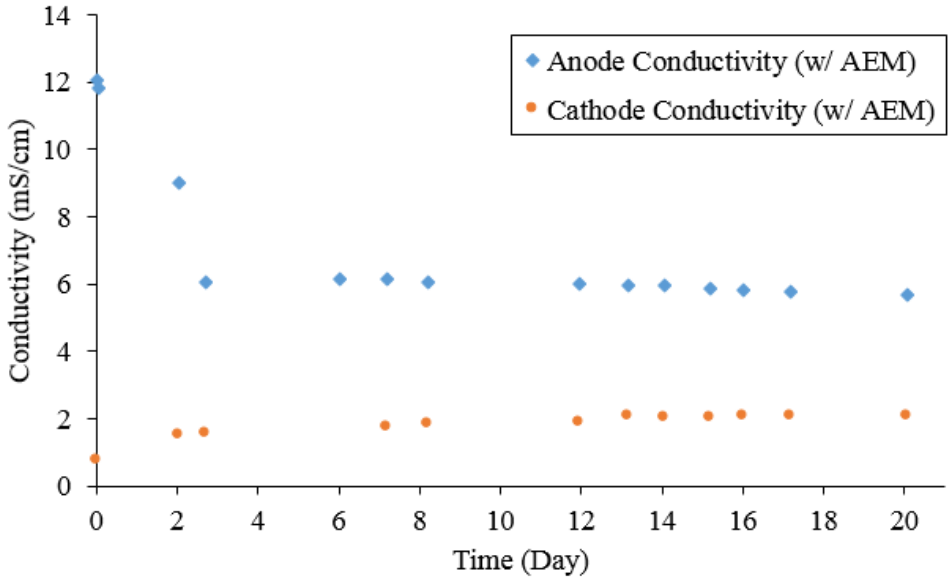

Figure 4.14: Anolyte and catholyte conductivity in the AEM-MEC.

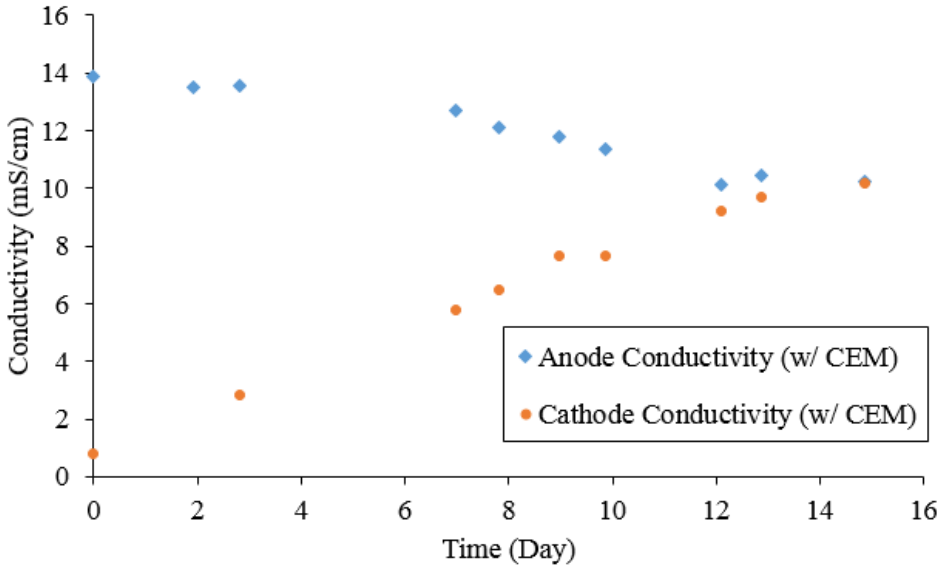

Figure 4.15: Anolyte and catholyte conductivity in the CEM-MEC.

The anolyte conductivity in the AEM-MEC was decreased and maintained at ~ 6 mS/cm. On the other hand, the catholyte conductivity increased slightly within 2 days of the operation (from 0.78 to 1.56 mS/cm) and remained relatively constant at 2 mS/cm. These results indirectly support the equilibrium of chemical concentrations achieved in the AEM-MEC. The anolyte conductivity in the CEM-MEC also increased with time from 13.9 (Day 1) to 10.25 (Day 15). The catholyte conductivity in the CEM-MEC increased noticeably over the course of the operation from 0.76 to 10.17 mS/cm. The increase in the catholyte conductivity would be attributed to the transport of the cations (i.e. Ca^{2+}, Mg^{2+}, and Na^{+}) from the anode the cathode.

4.2.4 H_2O_2 Concentration & H_2O_2 Conversion Efficiency

Figure 4.16 and Figure 4.17 presents cumulative H_2O_2 concentration and H_2O_2 conversion efficiency over time in the AEM-MEC and the CEM-MEC.

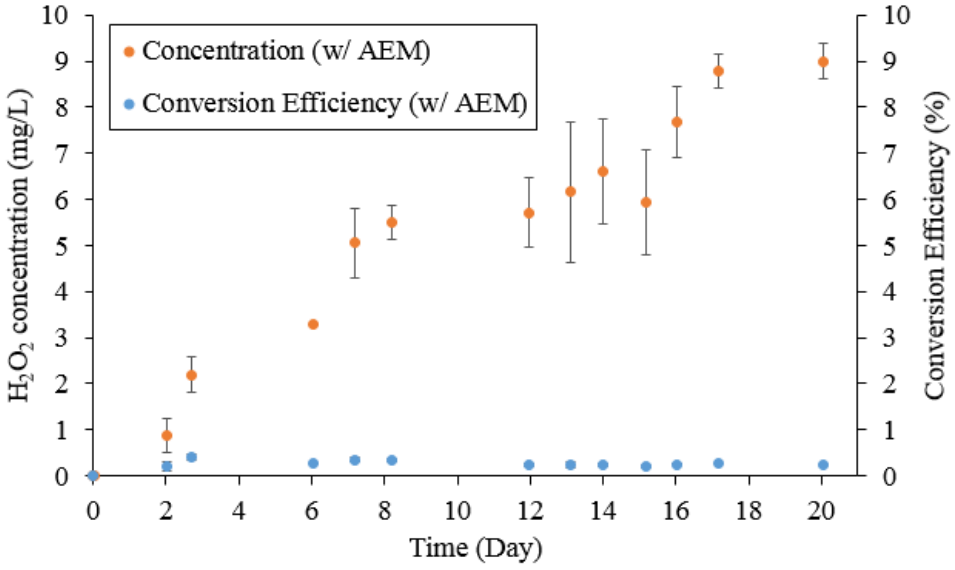

Figure 4.16: H_2O_2 concentration and H_2O_2 conversion efficiency in the AEM-MEC (bars represent standard deviation)

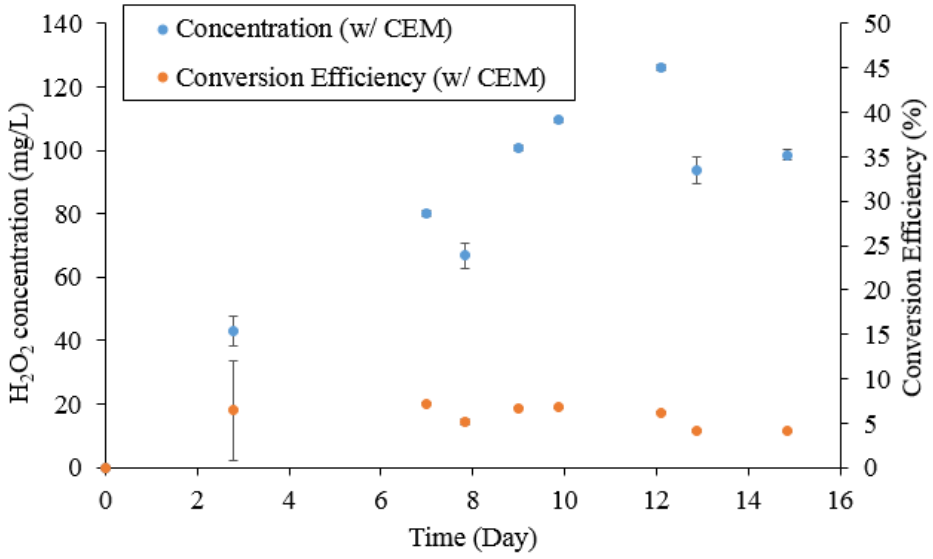

Figure 4.17: H_2O_2 concentration and H_2O_2 conversion efficiency in the CEM-MEC (bars represent standard deviation)

In the AEM-MEC, H_2O_2 was linearly generated with a cumulative H_2O_2 concentration of 9.0 ± 0.38 mg/L ($p = 0.007$) by the end of 20-day operation. The low H_2O_2 production in the AEM-MEC can be explained by the low current density (Figure 4.8). Also, low H_2O_2 conversion efficiency attributed to low H_2O_2 concentrations in the AEM-MEC, ranging between 0.20 ± 0.03 ($p = 0.048$) and 0.35 ± 0.05 % ($p = 0.050$) throughout the operation. High catholyte pH played a role in low H_2O_2 conversion efficiency in the AEM-MEC (Figure 4.11); high pH (pH>8) is reported to stimulate self-decomposition of H_2O_2 (Qiang, et al., 2002).

In accordance to the AEM-MEC, the CEM-MEC also showed the linear H_2O_2 generation with time; however, the CEM-MEC showed slightly better H_2O_2 production. The cumulative H_2O_2 concentration was 98.48 ± 1.6 mg/L ($p = 0.007$) at the end of the 15-day operation for the CEM-MEC. This resulted from higher H_2O_2 conversion efficiencies in the CEM-MEC than those in the AEM-MEC. The H_2O_2 conversion efficiency in the CEM-MEC ranged from 4.1 ± 0.07 ($p < 0.001$)

to 7.2 ± 0.09 % ($p = 0.006$). The higher H_2O_2 conversion efficiencies in the CEM-MEC than those in the AEM-MEC could be due to the continuous H^+ supply from the anode the cathode via the cation exchange membrane. It is interesting that the H_2O_2 production and H_2O_2 conversion efficiency in the large-scale MEC were considerably lower than those in the laboratory-scale MEC although the CEM-MEC and the laboratory-scale MEC had comparable catholyte pH (high pH > 8) and $E_{cathode}$ throughout the operations. These results indirectly support that substantially lower current density in the CEM-MEC than those in the laboratory-scale MEC was a key feature for the low H_2O_2 production in the pilot system. This suggests that improving the current density in MECs is inevitably essential for the successful implementation of the technology in large scale.

4.3 Conclusions

The research in MECs has advanced rapidly in recent years; however, it is still at an early stage for the practical implementation and only a few research groups attempted the operation of pilot-scale MECs. Among the pilot studies conducted in the past years, no pilot study targeted H_2O_2 production. In this study consisting of two phases (phase I: AEM-MEC and phase II: CEM-MEC), the pilot-scale MEC was operated on acetate synthetic wastewater to evaluate H_2O_2 production.

The operation of the pilot-scale MEC required a small voltage input from -0.35 to -1.90 V. The maximum current density of 0.94 and 0.96 A/m^2 were achieved in the AEM-MEC and the CEM-MEC, respectively. Low current densities resulted in low H_2O_2 production in the pilot-scale MEC; the highest cumulative H_2O_2 concentration was 98.48 ± 1.6 mg/L in the 16-day operation of the CEM-MEC and 9.0 ± 0.38 mg/L in the 20-day operation of the AEM-MEC. Low H_2O_2 conversion efficiency attributed to low H_2O_2 production in the pilot system; the highest H_2O_2 conversion

efficiency was 7.2 ± 0.09 % and 0.35 ± 0.05 % in the CEM-MEC and the AEM-MEC, respectively. The lower H_2O_2 conversion efficiency in the pilot-scale MEC would result from low current density and high pH (pH >8) in the cathode, which would favor self-decomposition of H_2O_2 and H_2O_2 reduction to H_2O.

Over the course of the operation, the major challenges associated with the membrane and the CGC were identified. Due to these challenges, a frequent maintenance work was required over each operation, adversely affecting the performance of the system. Also, the pilot-scale MEC would require modifications to its design for the issue of CO_2 trapping in order to resolve the acidification in the anode. In additional to those challenges, low current generation in the pilot-scale MEC also needs to be addressed in the future study in order to achieve the implementation of MECs in practical applications for H_2O_2 production.

5 Conclusions

This study was aimed to investigate the applicability of MECs to supplant the energy-intensive AO process for H_2O_2 production. Several conclusions were drawn from this study and presented in this chapter.

From the preliminary experiments that were designed to establish an optimal operating conditions for the cathode, the following conclusions were drawn:

- Compared to the GC, the CGC generated higher H_2O_2 due to higher H_2O_2 conversion efficiencies, which were 16, 12, 2.5 % (12, 0.2, and 0.3 % for the GC) at the $E_{cathode}$ of -0.4, -0.6, and -0.8 V, respectively.
- In the active aeration mode, the effect of the $E_{cathode}$ on ORRs was profound; O_2 reduction to H_2O was favored as the $E_{cathode}$ became more negative for the GC and the CGC.
- High H_2O_2 conversion efficiencies (30 to 65 %) with the passive aeration indicated that the aeration method favored O_2 reduction to H_2O_2 because it would provide higher O_2 concentration and compensate for the low solubility of O_2.
- In the passive aeration mode, the $E_{cathode}$ did not have a profound effect on H_2O_2 conversion efficiency and H_2O_2 conversion efficiency remained high as the $E_{cathode}$ was increased from -0.4 to -1.2 V.

In the following stage of the study, the lab-scale MEC was operated on two feeds at different HRTs and the followings conclusions were made:

- In the acetate-fed MEC, the current density and H_2O_2 production improved as the HRT was shortened. The highest current density of 8.0 ± 0.6 A/m^2 at the shortest HRT (2 hr) led to a cumulative H_2O_2 concentration of 843.50 ± 17.30 mg/L at 6 hr of cathode operation.

- High pH (pH > 8) in the cathode and accumulation of H_2O_2 with time accelerated H_2O_2 destruction, causing H_2O_2 conversion efficiency to drop with time.
- The current density deteriorated substantially when the lab-scale system was operated on domestic wastewater; the highest current density in the wastewater-MEC was 0.60 ± 0.05 A/m^2 at the HRT of 6 hrs.
- Low H_2O_2 production was observed in the wastewater-fed MEC due to the extremely low current densities. The maximum cumulative H_2O_2 concentration was 147.73 ± 1.98 mg/L at 24 hr of cathode operation.

In the last stage of the study, the applicability of the MEC was assessed for H_2O_2 production at pilot-scale when the system was equipped with an AEM and a CEM, and the following are the conclusions that were drawn:

- The maximum current density of 0.94 and 0.96 A/m^2 was achieved in the AEM-MEC and the CEM-MEC, respectively.
- Low current densities in the pilot-scale MEC resulted in low H_2O_2 production with the maximum cumulative H_2O_2 concentration of 9.0 ± 0.38 mg/L and 98.48 ± 1.6 mg/L in the 20-day operation of the AEM-MEC and the 15-day of the CEM-MEC, respectively. Also, low H_2O_2 conversion efficiencies were observed, ranging from 0.24 to 0.35 % and from 4.1 ± 0.07 to 7.2 ± 0.09 % in the AEM-MEC and the CEM-MEC, respectively.
- The anolyte pH in the AEM-MEC dropped below 6.5 in 21 days due to trapping of CO_2 that was produced from acetate oxidation. For the CEM-MEC, CO_2 lowered the anolyte pH. H^+ accumulation in the anode also decreased the anolyt pH, accelerating pH drop in the anode.

- The current design of the pilot-scale MEC requires a few modifications, such as membrane supporters and an outlet for the release of CO_2, for the minimal maintenance and the optimal performance.

6 Recommendations

This study showed that high H_2O_2 production in MECs was possible and exhibited its potential to supplant the AO process. However, it also exposed a number of the challenges that further research must focus on:

- Current density deteriorated substantially when the lab-scale MEC was operated on real wastewater. Therefore, it is essential for the further research to identify the parameters in real wastewater that adversely impact on current generation in MECs fed with real wastewater.
- The pilot-scale MEC generated low current and H_2O_2 although it was operated on acetate synthetic wastewater. Therefore, the research needs to focus on improving the current density in the pilot-scale MEC for the maximal H_2O_2 production.
- A novel design for large-scale MEC is required for the minimal maintenance and the optimal performance of the pilot systems by addressing the design challenges that were discussed, such as membrane expansion and CO_2 trapping.

References

Aelterman, P., S. Freguia, et al. (2008). "The anode potential regulates bacterial activity in microbial fuel cells." Applied Microbiology and Biotechnology **78**(3): 409-418.

Agladze, G. R., Tsurtsumia, G. S., Jung, B. I., Kim, J. S., & Gorelishvili, G. (2007). "Comparative study of hydrogen peroxide electro-generation on gas-diffusion electrodes in undivided and membrane cells". *Journal of applied electrochemistry*, *37*(3), 375-383.

An, J. and H.-S. Lee (2013). "Implication of endogenous decay current and quantification of soluble microbial products (SMP) in microbial electrolysis cells." RSC Advances **3**(33): 14021-14028.

Ando, Y. and T. Tanaka (2004). "Proposal for a new system for simultaneous production of hydrogen and hydrogen peroxide by water electrolysis." International Journal of Hydrogen Energy **29**(13): 1349-1354.

Andreozzi, R., V. Caprio, et al. (1999). "Advanced oxidation processes (AOP) for water purification and recovery." Catalysis Today **53**(1): 51-59.

APHA, AWWA, & WEF. (1992). *Standard Methods for the Examination of Water and Wastewater* (18th ed.). Wahington DC, USA.

Asghar, A., A. A. Abdul Raman, et al. (2014). "Recent advances, challenges and prospects of in situ production of hydrogen peroxide for textile wastewater treatment in microbial fuel cells." Journal of Chemical Technology & Biotechnology **89**(10): 1466-1480.

Bard, A. J. and L. R. Faulkner (2001). "Electrochemical methods: fundamentals and applications, 2nd." Hoboken: Wiley and Sons.

Brillas, E., F. Alcaide, et al. (2002). "A small-scale flow alkaline fuel cell for on-site production of hydrogen peroxide." Electrochimica Acta **48**(4): 331-340.

Campos-Martin, J. M., G. Blanco-Brieva, et al. (2006). "Hydrogen Peroxide Synthesis: An Outlook beyond the Anthraquinone Process." Angewandte Chemie International Edition **45**(42): 6962-6984.

Chae, K.-J., M.-J. Choi, et al. (2010). "Selective inhibition of methanogens for the improvement of biohydrogen production in microbial electrolysis cells." International Journal of Hydrogen Energy **35**(24): 13379-13386.

Cusick, R., B. Bryan, et al. (2011). "Performance of a pilot-scale continuous flow microbial electrolysis cell fed winery wastewater." Applied Microbiology and Biotechnology **89**(6): 2053-2063.

Dhar, B. R. and H.-S. Lee (2014). "Evaluation of limiting factors for current density in microbial electrochemical cells (MXCs) treating domestic wastewater." Biotechnology Reports **4**(0): 80-85.

Escapa, A., M. I. San Martin, et al. (2014). "POTENTIAL USE OF MICROBIAL ELECTROLYSIS CELLS (MECs) IN DOMESTIC WASTEWATER TREATMENT PLANTS FOR ENERGY RECOVERY." Frontiers in Energy Research **2**.

Feng, C.-H., F.-B. Li, et al. (2010). "Bio-Electro-Fenton Process Driven by Microbial Fuel Cell for Wastewater Treatment." Environmental Science & Technology **44**(5): 1875-1880.

Fu, L., S.-J. You, et al. (2010)[a]. "Degradation of azo dyes using in-situ Fenton reaction incorporated into H2O2-producing microbial fuel cell." Chemical Engineering Journal **160**(1): 164-169.

Fu, L., S.-J. You, et al. (2010)[b]. "Synthesis of hydrogen peroxide in microbial fuel cell." Journal of Chemical Technology & Biotechnology **85**(5): 715-719.

Gil-Carrera, L., A. Escapa, et al. (2013)[a]. "Microbial electrolysis cell scale-up for combined wastewater treatment and hydrogen production." Bioresource Technology **130**(0): 584-591.

Gil-Carrera, L., A. Escapa, et al. (2013)[b]. "Performance of a semi-pilot tubular microbial electrolysis cell (MEC) under several hydraulic retention times and applied voltages." Bioresource Technology **146**(0): 63-69.

Goldstein R, Smith W.Water & Sustainability (Volume 4): U.S Electricity Consumption for Water Supply & Treatment – The Next Half Century. Electric Power Research Institute, Inc. (EPRI); 2002.

Guo, T. X., Zhao, Y., Ma, S. C., & Liu, S. T. (2013). "Decomposition Characteristics of Hydrogen Peroxide in Sodium Hydroxide Solution". *Advanced Materials Research, 610*, 359-362.

Kepa, U., E. Stanczyk-Mazanek, et al. (2008). "The use of the advanced oxidation process in the ozone + hydrogen peroxide system for the removal of cyanide from water." Desalination **223**(1–3): 187-193.

Kim, J. R., S. Cheng, et al. (2007). "Power Generation Using Different Cation, Anion, and Ultrafiltration Membranes in Microbial Fuel Cells." Environmental Science & Technology **41**(3): 1004-1009.

Ksibi, M. (2006). "Chemical oxidation with hydrogen peroxide for domestic wastewater treatment." Chemical Engineering Journal **119**(2–3): 161-165.

Lee, H.-S., C. I. Torres, et al. (2009). "Effects of Substrate Diffusion and Anode Potential on Kinetic Parameters for Anode-Respiring Bacteria." Environmental Science & Technology **43**(19): 7571-7577.

Logan, B. (2010). "Scaling up microbial fuel cells and other bioelectrochemical systems." Applied Microbiology and Biotechnology **85**(6): 1665-1671.

Logan, B. E. and K. Rabaey (2012). "Conversion of Wastes into Bioelectricity and Chemicals by Using Microbial Electrochemical Technologies." Science **337**(6095): 686-690.

Modin, O., & Fukushi, K. (2012). Development and testing of bioelectrochemical reactors converting wastewater organics into hydrogen peroxide. *Water Science & Technology*, *66*(4), 831-836.

Modin, O. and K. Fukushi (2013). "Production of high concentrations of H2O2 in a bioelectrochemical reactor fed with real municipal wastewater." Environmental Technology **34**(19): 2737-2742.

Nogueira, R. F. P., M. C. Oliveira, et al. (2005). "Simple and fast spectrophotometric determination of H2O2 in photo-Fenton reactions using metavanadate." Talanta **66**(1): 86-91.

Panizza, M. and G. Cerisola (2008). "Electrochemical generation of H_2O_2 in low ionic strength media on gas diffusion cathode fed with air." Electrochimica Acta **54**(2): 876-878.

Parameswaran, P., C. I. Torres, et al. (2009). "Syntrophic interactions among anode respiring bacteria (ARB) and Non-ARB in a biofilm anode: electron balances." Biotechnology and bioengineering **103**(3): 513-523.

Pikaar, I., B. Virdis, et al. (2014). "Wastewater Treatment (Microbial Bioelectrochemical) and Production of Value-Added By-Products." Encyclopedia of Applied Electrochemistry: 2111-2117.

Pozzo, A. D., L. D. Palma, et al. (2005). "An experimental comparison of a graphite electrode and a gas diffusion electrode for the cathodic production of hydrogen peroxide." Journal of Applied Electrochemistry **35**(4): 413-419.

Qiang, Z., J.-H. Chang, et al. (2002). "Electrochemical generation of hydrogen peroxide from dissolved oxygen in acidic solutions." Water Research **36**(1): 85-94.

Rabaey, K. and W. Verstraete (2005). "Microbial fuel cells: novel biotechnology for energy generation." Trends in biotechnology **23**(6): 291-298.

Reis, R. M., A. A. G. F. Beati, et al. (2011). "Use of Gas Diffusion Electrode for the In Situ Generation of Hydrogen Peroxide in an Electrochemical Flow-By Reactor." Industrial & Engineering Chemistry Research **51**(2): 649-654.

Rozendal, R. A., H. V. M. Hamelers, et al. (2008). "Towards practical implementation of bioelectrochemical wastewater treatment." Trends in biotechnology **26**(8): 450-459.

Rozendal, R. A., E. Leone, et al. (2009). "Efficient hydrogen peroxide generation from organic matter in a bioelectrochemical system." Electrochemistry Communications **11**(9): 1752-1755.

Samanta, C. (2008). "Direct synthesis of hydrogen peroxide from hydrogen and oxygen: An overview of recent developments in the process." Applied Catalysis A: General **350**(2): 133-149.

Sleutels, T. H. J. A., H. V. M. Hamelers, et al. (2011). "Effect of mass and charge transport speed and direction in porous anodes on microbial electrolysis cell performance." Bioresource Technology **102**(1): 399-403.

Song, C. and J. Zhang (2008). Electrocatalytic oxygen reduction reaction. PEM fuel cell electrocatalysts and catalyst layers, Springer**:** 89-134. Sleutels, T. H. J. A., H. V. M. Hamelers, et al. (2011). "Effect of mass and charge transport speed and direction in porous anodes on microbial electrolysis cell performance." Bioresource Technology **102**(1): 399-403.

Torres, C. I., A. Kato Marcus, et al. (2008). "Proton transport inside the biofilm limits electrical current generation by anode-respiring bacteria." Biotechnology and Bioengineering **100**(5): 872-881.

Torres, C. I., R. Krajmalnik-Brown, et al. (2009). "Selecting Anode-Respiring Bacteria Based on Anode Potential: Phylogenetic, Electrochemical, and Microscopic Characterization." Environmental Science & Technology **43**(24): 9519-9524.

Yamanaka, I. (2008). "Direct Synthesis of H_2O_2 by a H_2/O_2 Fuel Cell." Catalysis Surveys from Asia **12**(2): 78-87.

Yamanaka, I. and T. Murayama (2008). "Neutral H_2O_2 Synthesis by Electrolysis of Water and O_2." Angewandte Chemie **120**(10): 1926-1928.

Zhang, F., Z. Ge, et al. (2013). "Long-Term Performance of Liter-Scale Microbial Fuel Cells Treating Primary Effluent Installed in a Municipal Wastewater Treatment Facility." Environmental Science & Technology **47**(9): 4941-4948.

Zhang, L., P. De Schryver, et al. (2008). "Chemical and biological technologies for hydrogen sulfide emission control in sewer systems: A review." Water Research **42**(1–2): 1-12.

Zhang, Y. and I. Angelidaki (2014). "Microbial electrolysis cells turning to be versatile technology: Recent advances and future challenges." Water Research **56**(0): 11-25.

Appendix A: H_2O_2 Evolution in the laboratory-scale MEC fed with acetate

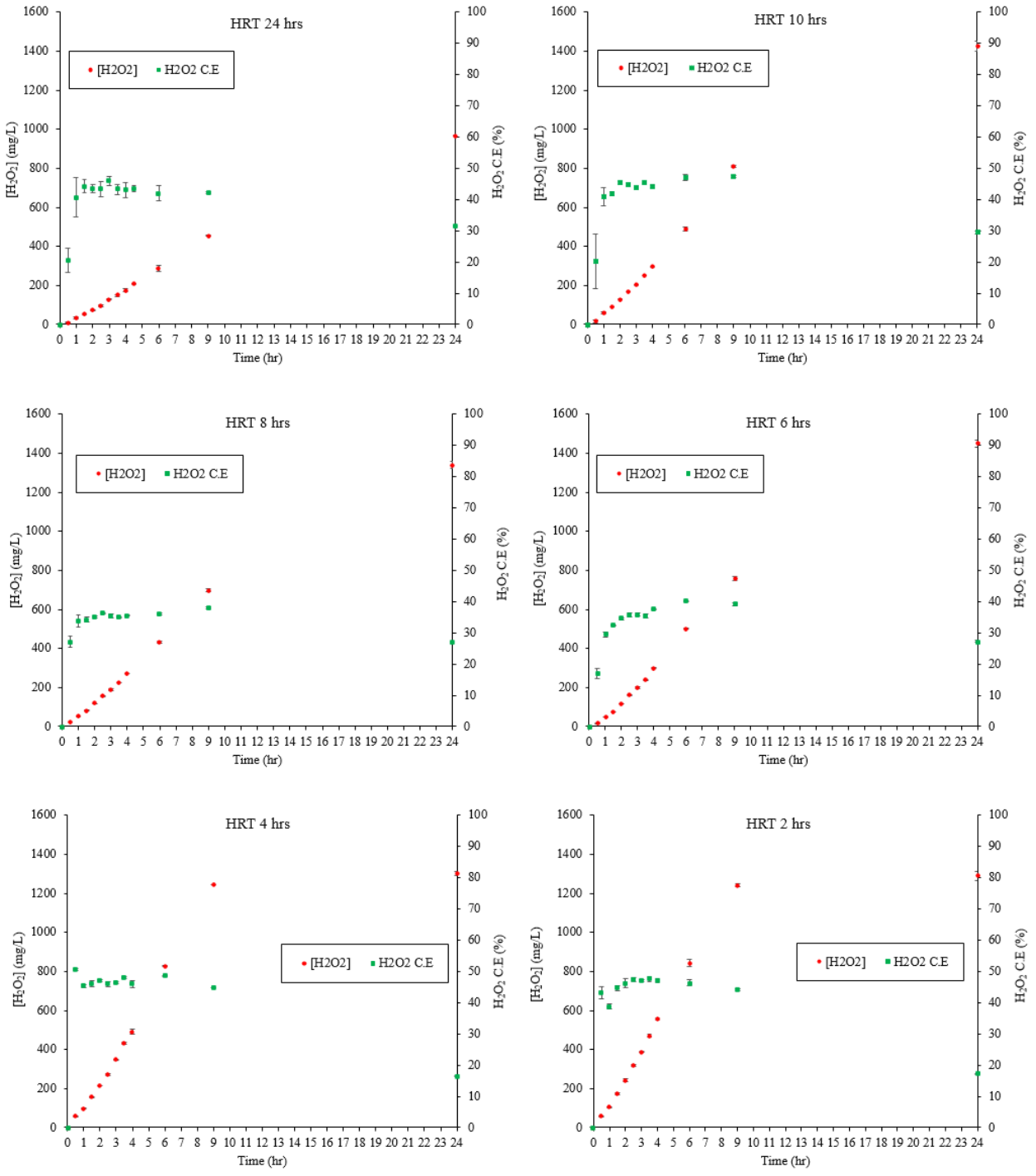

Figure A.0.1: H_2O_2 concentration and conversion efficiency evolution in the laboratory-scale MEC fed with acetate at different HRTs (bars represent standard deviation).